NRL Report 9141

AD-A200 929   DTIC FILE COPY

Refocusing a Radio Telescope to Image Sources
Within the Nearfield of the Antenna Array

WILLIAM H. CARTER

Space Systems Technology Department

October 17, 1988

DTIC
ELECTE
DEC 0 5 1988
S
E
D

88 12 2 009

REPORT DOCUMENTATION PAGE

Form Approved
OMB No. 0704-0188

1a. REPORT SECURITY CLASSIFICATION	1b. RESTRICTIVE MARKINGS
Unclassified	

2a. SECURITY CLASSIFICATION AUTHORITY	3. DISTRIBUTION/AVAILABILITY OF REPORT
2b. DECLASSIFICATION/DOWNGRADING SCHEDULE	Approved for public release; distribution unlimited.

4. PERFORMING ORGANIZATION REPORT NUMBER(S)	5. MONITORING ORGANIZATION REPORT NUMBER(S)
NRL Report 9141	

6a. NAME OF PERFORMING ORGANIZATION	6b. OFFICE SYMBOL (If applicable)	7a. NAME OF MONITORING ORGANIZATION
Naval Research Laboratory	Code 8304	Naval Research Laboratory

6c. ADDRESS (City, State, and ZIP Code)	7b. ADDRESS (City, State, and ZIP Code)
Washington, DC 20375-5000	Washington, DC 20375-5000

8a. NAME OF FUNDING/SPONSORING ORGANIZATION	8b. OFFICE SYMBOL (If applicable)	9. PROCUREMENT INSTRUMENT IDENTIFICATION NUMBER
Office of Naval Research		

8c. ADDRESS (City, State, and ZIP Code)	10. SOURCE OF FUNDING NUMBERS			
	PROGRAM ELEMENT NO	PROJECT NO	TASK NO	WORK UNIT ACCESSION NO
Arlington, VA 22217-5000	51153N	RR01402		DN 158-096

11. TITLE (Include Security Classification)

Refocusing a Radio Telescope to Image Sources Within the Nearfield of the Antenna Array

12. PERSONAL AUTHOR(S)
Carter, William H.

13a. TYPE OF REPORT	13b. TIME COVERED FROM _____ TO _____	14. DATE OF REPORT (Year, Month, Day) 1988 October 17	15. PAGE COUNT 44

16. SUPPLEMENTARY NOTATION

17. COSATI CODES			18. SUBJECT TERMS (Continue on reverse if necessary and identify by block number)
FIELD	GROUP	SUB-GROUP	Radio astronomy, Coherency theory, Radio telescope
			Fraunhofer, Nearfield

19. ABSTRACT (Continue on reverse if necessary and identify by block number)

A theory is developed from three forms of the Fraunhofer approximation that describes a method for refocusing a radio telescope to image sources that are within the nearfield of the antenna array. In the first section the Fraunhofer approximations of the first, second, and third kinds are derived and studied in applications to the propagation of a scalar field amplitude from sources to detectors. In the second section these approximations are applied to the propagation of the cross-spectral density function of coherence theory. Important differences between the conditions for validity and the mathematical structure of these three approximations are described. In the final section a theoretical model is developed to describe the operation of a radio telescope using the theory developed in the first two sections. This model is used to develop a method for refocusing a radio telescope to image sources that are within the nearfield of the antenna array. Two methods for refocusing the telescope are described that would require no modification to most existing telescopes but would require some modifications to the data processing software.

20. DISTRIBUTION/AVAILABILITY OF ABSTRACT	21. ABSTRACT SECURITY CLASSIFICATION
☒ UNCLASSIFIED/UNLIMITED ☐ SAME AS RPT ☐ DTIC USERS	Unclassified

22a. NAME OF RESPONSIBLE INDIVIDUAL	22b. TELEPHONE (Include Area Code)	22c. OFFICE SYMBOL
William H. Carter	(202) 767-2453	Code 8304

DD Form 1473, JUN 86   Previous editions are obsolete.   SECURITY CLASSIFICATION OF THIS PAGE

S/N 0102-LF-014-6603

i

CONTENTS

REFOCUSING A RADIO TELESCOPE TO IMAGE SOURCES WITHIN THE NEARFIELD OF THE ANTENNA ARRAY

1 THREE FRAUNHOFER APPROXIMATIONS FOR THE PROPAGATION OF FIELD AMPLITUDE

1.1 Introduction

The Fraunhofer approximation is one of the most useful mathematical tools used in optics. It is widely used by optical engineers to model systems and by researchers to model physical phenomena. The Fraunhofer approximation is also widely used by physicists in connection with radiation problems, and by electrical engineers to deal with antennas and electromagnetic wave propagation. However, it is not so well known that the Fraunhofer approximation as usually used in these different disciplines is different in some important ways. These differences and the resulting capabilities to model phenomena have given rise to their different use.

In Section 1 we examine applications of three Fraunhofer approximations to simple field theory, where we deal with the propagation of a (generally complex) scalar field amplitude from sources to detectors. In Section 2 we extend the study to applications of the Fraunhofer approximations to second-order coherence theory.

The present section derives these three forms of the Fraunhofer approximation by using similar notation to simplify comparison. Then each of the three kinds of Fraunhofer approximations are examined and compared to the others to point out the differences in the conditions for validity, mathematical structure, and unique capabilities in application.

1.2 Detector in the Farfield of the Source Distribution

First we will briefly review the Fraunhofer approximation as it usually appears in radiation problems in mathematical physics [1, Section 9.1]. Here we establish a specific set of conditions and notation to contrast this formulation with different, but similar Fraunhofer approximations frequently used in optics and in electrical engineering.

Consider the configuration shown in Fig. 1 with a three-dimensional source distribution localized to a region about the origin and radiating an electromagnetic field toward a detector located a distance R from the origin in any direction. We assume that the source is a primary, three-dimensional source distribution so that a typical scalar, monochromatic, Cartesian component of the electromagnetic field $\psi(\mathbf{x})$ (with suppressed exp $(-i\omega t)$ time dependence) is related to the source distribution $\rho(\mathbf{x})$ by the scalar Helmholtz equation

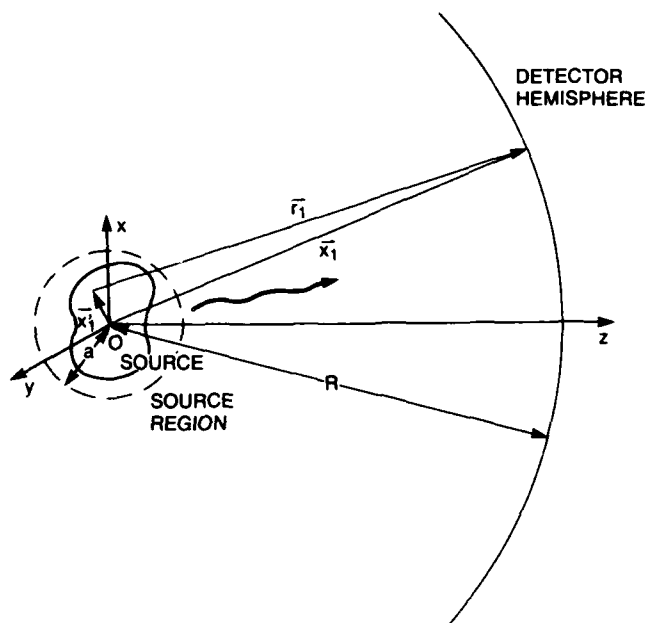$$(\nabla^2 + k^2)\psi(\mathbf{x}) = -4\pi\rho(\mathbf{x}) \tag{1}$$

Fig. 1 — Configuration for the Fraunhofer approximation of the first kind with the detector in the farfield in any direction from a three-dimensional source distribution about the origin

[2, Eq. (2.8)], where $k = 2\pi/\lambda = \omega/c$. The solution to Eq. (1) that represents an outgoing wave at infinity is

$$\psi(\mathbf{x}_1) = \iiint\limits_{-\infty}^{\infty} \rho(\mathbf{x}_1') \exp{(ik\,|\mathbf{r}_1|)}/|\mathbf{r}_1|\,d^3\mathbf{x}_1', \tag{2}$$

where $\mathbf{x}_1'$ and $\mathbf{x}_1$ represent radius vectors from the origin to the source and field points respectively and $\mathbf{r}_1$ represents the vector $\mathbf{x}_1 - \mathbf{x}_1'$, as shown in Fig. 1. Following a well-known procedure we expand $|\mathbf{r}_1|$ into the binomial series

$$|\mathbf{r}_1| = \sqrt{(x_1 - x_1')^2 + (y_1 + y_1')^2 + (z_1 - z_1')^2}$$

$$\sim R - (\mathbf{x}_1 \cdot \mathbf{x}_1')/R + O(|\mathbf{x}_1'|^2/R), \tag{3}$$

where $R = |\mathbf{x}_1|$. If the source distribution is confined to a spherical region within a radius a of the origin and the detectors are all far outside the Rayleigh range of the source so that

$$R >> ka^2, \tag{4}$$

then we may approximate the value of $|\mathbf{r}_1|$ in the denominator of the kernel of the integral in Eq. (2) by the first term in Eq. (3) and the value of $|\mathbf{r}_1|$ in the phase by the first two terms to obtain the Fraunhofer approximation of the first kind given by

$$\psi(R\mathbf{s}) = \exp{(ikR)}/R \iiint\limits_{-\infty}^{\infty} \rho(\mathbf{x}_1') \exp{(-ik\mathbf{s} \cdot \mathbf{x}_1')}d^3\mathbf{x}_1', \tag{5}$$

2

where s is the unit vector from the origin to the field point at x_1 and x_1' is the three-dimensional radius vector from the origin to a point in the source distribution.

Equation (5) gives the Fraunhofer approximation for the radiation field from a primary, three-dimensional source distribution about the origin as it often appears in physics problems [1, Eq. (9.8)]. In optical diffraction problems a similar but somewhat different form of Fraunhofer approximation is usually used [3, Section 8.3.3]. Instead of a primary, three-dimensional source distribution a planar, secondary source distribution is usually assumed and the field is limited to the $z \geq 0$ half space. In such problems we assume that the primary sources are distributed over the $z < 0$ half space and radiate toward the $z = 0$ plane. We assume that owing either to the nature of the source distribution or to an aperture in the $z = 0$ plane the field in this plane vanishes outside of some domain within a radius b of the origin, as shown in Fig. 2. Then this boundary condition for the field over the $z = 0$ plane $\psi^{(0)}(x_1')$ is treated as a secondary source distribution.
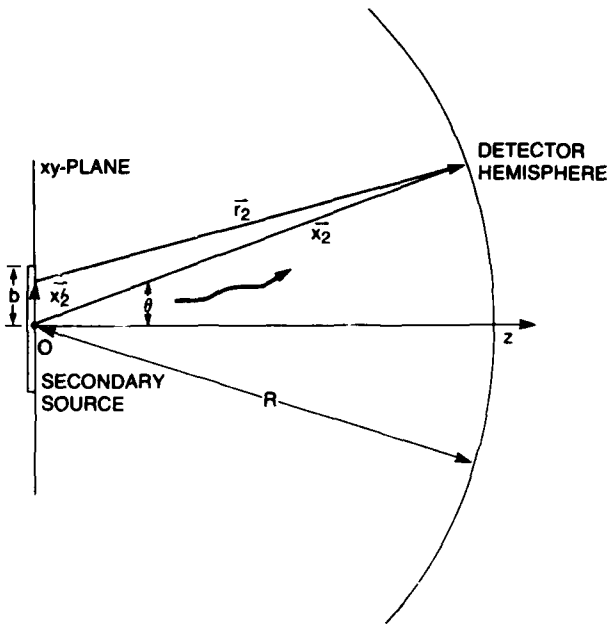

Fig. 2 — Configuration for the Fraunhofer approximation of the second kind with the detector in the farfield in the $z \geq 0$ half space of a two-dimensional source distribution over the $z = 0$ plane near the origin

For a secondary source distribution the homogeneous Helmholtz equation describes the field over the $z > 0$ half space [4, Section 3.2]. A well-known solution [4, Section 3.4] of this equation for the field over the detectors is given by the Rayleigh integral

$$\psi(x_2) = -1/2\pi \iint_{-\infty}^{\infty} \psi^{(0)}(x_2')\partial/\partial z_2[\exp{(ik\,|r_2|)}/|r_2|]d^2x_2', \qquad (6)$$

where x_2 and x_2' are the radius vectors from the origin to the field point at the detectors and the source point in the $z = 0$ plane, respectively, and r_2 is the vector $x_2 - x_2'$, as shown in Fig. 2. If we assume that $k\,|r_2|$ is sufficiently large, then we can make the approximation

$$-\partial/\partial z_2[\exp{(ik\,|r_2|)}/|r_2|] = (-z_2/|r_2|)(ik - 1/|r_2|)[\exp{(ik\,|r_2|)}/|r_2|]$$

$$\sim (-ikz_2/|r_2|)[\exp{(ik\,|r_2|)}/|r_2|]. \qquad (7)$$

3

It is useful to expand

$$|\mathbf{r}_2| = \sqrt{(x_2 - x_2')^2 + (y_2 - y_2')^2 + z_2^2}$$

$$\sim R - (\mathbf{x}_2 \cdot \mathbf{x}_2')/R + O(|\mathbf{x}_2'|^2/R), \tag{8}$$

where R has the same meaning as in Eq. (3). If we also assume that the secondary source in the $z = 0$ plane is confined to the interior of a circle of radius b around the origin and that the detectors are all located outside of the Rayleigh range of the source distribution so that

$$R >> kb^2, \tag{9}$$

then upon substitution from Eq. (7) into Eq. (6) and replacing the value of $|\mathbf{r}_2|$ in the denominator of the kernel with the first term in Eq. (8) and the value in the phase by the first two terms in Eq. (8) we have the Fraunhofer approximation of the second kind given by

$$\psi(R\mathbf{s}) = (-ik/2\pi) \cos\theta \, (\exp(ikR)/R) \int\int_{-\infty}^{\infty} \psi^{(0)}(\mathbf{x}_2')(\exp(-ik\mathbf{s} \cdot \mathbf{x}_2')d^2\mathbf{x}_2', \tag{10}$$

where $\mathbf{x}_2'$ is a vector within the $z = 0$ plane, i.e., $\mathbf{x}_2' = (x_2', y_2', 0)$, s is the three-dimensional unit vector from the origin in the direction of $\mathbf{x}_2$, and θ is the angle that s makes with the $+z$ axis.

The Fraunhofer formula Eq. (10), for the field owing to a secondary source, is frequently employed in optics to deal with diffraction problems [4, Eq. (4.13)]. The relation given in Eq. (5) for a three-dimensional, primary source differs from Eq. (10) more than one might suppose in view of the similarity of their derivations. The main mathematical differences, which will be examined in more detail in the next subsection, arise from the fact that the integral appearing in Eq. (5) is three-dimensional unlike the integral that appears in Eq. (10) and that s is a unit vector so that the three-dimensional Fourier transform appearing in Eq. (5) is evaluated only on a sphere of unit radius in (s_x, s_y, s_z) space. It is well known that these mathematical properties give rise to some very important properties of radiating source distributions, and are of particular interest when dealing with inverse problems. This subject will be discussed further in Subsection 1.4.

A third form of the Fraunhofer approximation exists that is frequently used by electrical engineers in dealing with antenna problems. It is also closely related to the Fraunhofer approximations appearing in Eqs. (5) and (10) but employs a significantly different set of assumptions and, therefore, has very different applications. We present a brief derivation of this Fraunhofer approximation to establish a precise set of conditions and notation before we consider these different formulations in more detail.

1.3 Source Distribution in the Farfield of the Detector Array

Figure 3 shows a configuration with a distribution of detectors located near the origin in the $z = 0$ plane that receive electromagnetic radiation from sources located a distance R from the origin in the $z \geq 0$ half space. Consider only a secondary source distribution (i.e., a boundary condition for the field over the hemisphere) rather than a true primary source distribution. Comparison of Figs. 2 and 3 shows that the two configurations are identical except for interchanging the positions of the sources and the detectors. Because of this similarity the fields at the sources and detectors can be related by using Eq. (10) and a well-known reciprocity theorem from antenna theory.
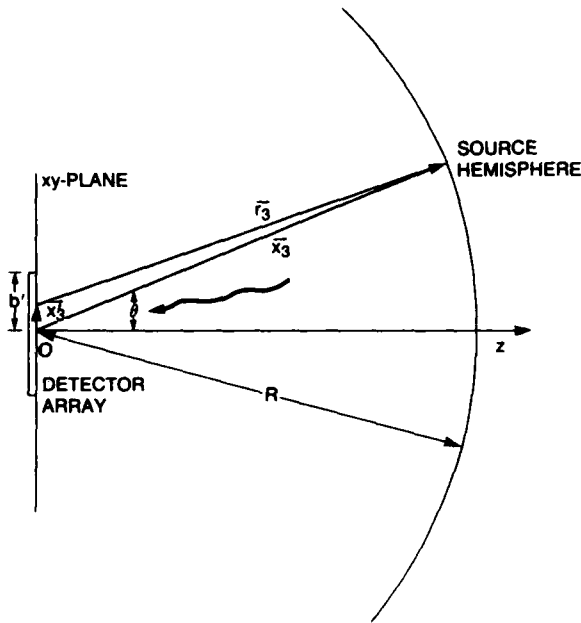
4

Fig. 3 — Configuration for the Fraunhofer approximation of the third kind with the sources outside of the Rayleigh range in the $z \geq 0$ half space of a two-dimensional detector array over the $z = 0$ plane near the origin

This reciprocity theorem [5, Section 10.2] leads to the well-known conclusion that the transmitting and receiving patterns of any antenna are the same. This theorem can be applied directly to transmitting patterns such as that given by Eq. (10) to give the equivalent receiving pattern of a detector array over the $z = 0$ plane. Thus, if we assume that the detectors are all confined to a region of the $z = 0$ plane within a circle of radius b' from the origin and that the sources of the field all are outside of the Rayleigh range of the source distribution, i.e.,

$$R >> kb'^2, \tag{11}$$

then Eq. (10) can be reinterpreted as an inverse propagation integral (after taking the complex conjugate of the kernel as discussed in Appendix A). Thus we obtain the field at a particular source point $\psi(\mathbf{x}_3)$ in the farfield of the detector as a function of field distribution $\psi^{(0)}(\mathbf{x}_3')$ over the detectors in the $z = 0$ plane.

It is well known that the Fraunhofer approximation of the second kind cannot simply be inverted to completely determine the source distribution over the $z = 0$ plane from measurements of the farfield. As discussed in detail in Subsection 1.4, this results from the fact that s is a unit vector that is only defined in Eq. (10) for directions from the origin into the $z \geq 0$ half space. However, this inversion problem disappears when Eq. (10) is reinterpreted by use of the reciprocity theorem to be a receiving, rather than a transmitting, antenna pattern and the sources of the field are defined to be located only in directions from the origin to the $z \geq 0$ half space, instead of on the $z = 0$ plane. Since the integral in Eq. (10) is a Fourier transform and since the function $\psi(R\mathbf{s})$ is defined to be nonvanishing only for s into the $z \geq 0$ half space (see Subsection 1.4), Eq. (10) can be easily inverted to give the Fraunhofer approximation of the third kind

$$\psi^{(0)}(\mathbf{x}_3) = (-ik/2\pi) \iint_{s_x^2 + s_y^2 \leq 1} [\psi(R\mathbf{s}) \exp(ikR)/R] \exp(-ik\mathbf{s} \cdot \mathbf{x}_3) R^2 (ds_x ds_y / s_z) \tag{12}$$

where $s = (s_x, s_y, s_z)$ is the radius vector from the origin to the source point at x_3 and x_3' is the radius vector from the origin to a point within the detector array. In Eq. (12) R is generally a function of s since we have had to make no mathematical restriction that the surface containing the sources be exactly hemispherical. Thus $R(s)$ cannot be taken outside of the integrals in Eq. (12).

The Fraunhofer formulas (Eqs. (5), (10), and (12)) do not have the same conditions for validity. The Fraunhofer approximations given by Eqs. (5) and (10) require that the source distribution be localized about the origin of coordinates and that the detectors all be in the farfield of the source distribution. For Eq. (5) the detector may be in any direction from the source; however, in Eq. (10) the detector must be located in the $z \geq 0$ half space. The different Fraunhofer formulation given by Eq. (12) requires that the detectors all be localized about the origin of coordinates and that the sources all be in the farfield of the detector array within the $z \geq 0$ half space. Thus the conditions for Eq. (10) are reciprocal to those for Eq. (12). Sometimes both the source distribution and the detector array are localized and are each in the farfield of the other so that these formulas differ only by a coordinate transformation from the origin within the source distribution to the origin within the detector array. However, this is generally not the case. Usually only one set of conditions is met so that only one of the Fraunhofer approximations is valid.

1.4 Differences Between Fraunhofer Approximations

As we noted, the three kinds of Fraunhofer approximations that we derived are different in some significant respects. We now consider them one at a time and point out some of their unique features.

Only the Fraunhofer approximation of the first kind in Eq. (5), involves a three-dimensional Fourier transform, which has some interesting consequences. Although the transform is three dimensional, the domain of $\psi(Rs)$ in Eq. (5) is only two dimensional. Since $s = (s_x, s_y, s_z)$ is a unit vector, its components are related by

$$s_x^2 + s_y^2 + s_z^2 = 1. \tag{13}$$

Thus the Fourier transform in Eq. (5) has clear physical meaning only for values of (s_x^2, s_y^2, s_z^2) over the surface of a sphere in s space. As a consequence, the farfield radiation from a three-dimensional source distribution is completely specified by only the spatial Fourier components of the source that have a period of one wavelength [6, Theorem I]. This property has proven useful in studying the question of nonradiating source distributions [6-10], scattering problems [11], and inverse scattering [12]. It appears likely that similar formulations could also be applied to phase matching problems. These physical properties of three-dimensional source distributions are not described by the Fraunhofer approximations of the second or third kinds.

Another interesting consequence of the three-dimensional integral in Eq. (5) involves an important class of inverse problems. These inverse problems employ measurements of farfield data to calculate the source distribution. We noted from Eq. (5) that farfield measurements give the Fourier transform of the three-dimensional source distribution only over the sphere of unit radius from the origin in a three-dimensional s space. To determine the source distribution for an arbitrary source by Fourier inversion of this data, the data would have to be known everywhere over s space. Some special cases are known for which farfield measurements are sufficient to reconstruct the source distributions. In scattering problems using the first Born approximation, for example, the source distribution represents a product of the known incident field and the scattering potential of the scatterers. Therefore, the scattering potential can be computed from a series of farfield measurements with different incident fields [13, 14].

6

The Fraunhofer approximation of the second kind given by Eq. (10) is different in two obvious ways from Eq. (5). Equation (10) contains constant and angle factors that result from the use of a secondary source distribution and a two-dimensional Fourier transform.

In Eq. (10) the Fourier transform is from the source plane (x'_2, y'_2) to the plane (s_x, s_y), where the third component of the unit vector s is given by

$$s_z = \cos \theta = \sqrt{1 - s_x^2 - s_y^2}, \text{ if } s_x^2 + s_y^2 \leq 1. \tag{14}$$

Fourier components of $\psi^{(0)}(x'_2)$ inside of the unit circle in Eq. (14) for which s_z is defined are called low-frequency spatial frequency components of the source and those outside are called high spatial frequency components.

This difference in dimensionality gives rise to the description of some interesting physical phenomena that are not described by the Fraunhofer approximation of the first kind in Eq. (5). An arbitrary source distribution contains high spatial frequency components outside of the unit radius in (s_x, s_y) space for which s_z is defined in Eq. (14). These high-frequency spatial frequency components have no effect on the farfield in any direction from the origin into the $z > 0$ half space. They are associated with evanescent plane waves that do not propagate into the farfield. It is possible to reconstruct the source distribution by using only the low-frequency spatial frequency components that are available from farfield measurements. However, the use of only low-frequency components results in a spatial resolution limit similar to that imposed by a diffraction limited lens $(NA = 1)$ to detail within the source distribution separated by intervals larger than a wavelength.

The Fraunhofer approximation of the third kind in Eq. (12) is different from that of the second kind in Eq. (10) in that the Fourier transform is from the s space to x'_3 space instead of the other way around. In Eq. (12) it is the sources that lie in directions away from the origin in the $z \geq 0$ half space and the detectors of the field that are in the $z = 0$ plane. The range of integration in Eq. (12) is only over real angles into the $z \geq 0$ half space so that the x and y components of s are bounded to the interior of the unit circle, as given by Eq. (14). Thus from Eq. (12) we see that the field over the $z = 0$ plane contains no spatial frequency components with periods smaller than a wavelength. Furthermore, by using a well-known theorem of Fourier analysis we know that the field over the $z = 0$ plane can be extended as an entire function of complex x'_3. Since the secondary source distribution is only defined physically for x and y components of s within the unit circle we can define the function to be zero elsewhere. With this definition there is no problem in inverting the Fourier transform in Eq. (10), which is interpreted as a receiving antenna pattern, to obtain Eq. (12). A consequence of these properties of the Fourier transform in Eq. (12) is that there appears to be no limitation in the angular resolution to which the source distribution can be calculated other than that arising from the limitation on the size of the detector array in the $z = 0$ plane.

Both the Fraunhofer approximations of the first and second kinds are valid only if the detectors are in the farfield of the source, i.e., the source distribution must be bounded so that it has a well-defined Rayleigh range, and the detector must be well outside of this Rayleigh range. In many important applications the source distribution is either not bounded or too large for this approximation. A radio antenna is an example. Here, the domain for the source distribution might completely surround the antenna. However, if the detector, like a radio antenna, is bounded, then it has a Rayleigh range itself and for sources outside of this Rayleigh range the Fraunhofer approximation of the third kind holds.

An important difference in the application of the Fraunhofer approximations of the second and third kinds, which both involve calculating the field from a known planar source distribution, can be

shown by use of an example. Consider a planar source distribution localized within a circle of radius b about an origin at O in the plane P in Fig. 4. Assume that it is radiating toward a planar detector array localized within a radius b' of an origin O' in the plane P' a distance D from P.
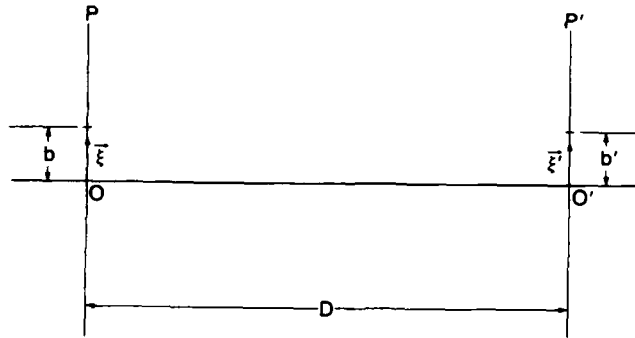

Fig. 4 — Notation for the example contrasting calculations performed using the Fraunhofer approximations of the second and third kinds

If b and R satisfy Eq. (9) so that Eq. (10) is a valid approximation, then to calculate the field over the detector array from a known source distribution, we perform a two-dimensional Fourier transform of the source distribution data, multiply the data by the constants and s-dependent factors outside of the integral in Eq. (10), and finally transform from angular to linear coordinates $\overline{\xi}'$ within the P' plane, i.e.,

$$\xi'_x = D(s_x/\sqrt{1 - s_x^2 - s_y^2})$$

$$\xi'_y = D(s_y/\sqrt{1 - s_x^2 - s_y^2}). \tag{15}$$

Figure 5(a) summarizes these steps.

If instead b' and R satisfy Eq. (11) so that Eq. (12) is a valid approximation, then to calculate the field over the plane P' from a known source distribution we must use a different procedure. First we transform the source distribution from linear coordinates $\overline{\xi}$ in the P plane into the angular coordinates from the origin at O', i.e.,

$$s_x = \xi_x/\sqrt{D^2 + \xi_x^2 + \xi_y^2}$$

and

$$s_y = \xi_y/\sqrt{D^2 + \xi_x^2 + \xi_y^2}. \tag{16}$$

Next we multiply the data by the s-dependent factors, and finally we Fourier transform the resulting data over the (s_x, s_y) plane to obtain the field over the $\overline{\xi}'$ plane. Figure 5(b) shows this procedure. Study of this figure readily shows the differences in the two procedures.

Finally we consider the interesting case for which b, b', and R satisfy both Eqs. (9) and (11) so that Eqs. (10) and (12) are both valid approximations. For this case either processing scheme shown

| MEASURE THE SOURCE DISTRIBUTION DIRECTLY | → | FOURIER TRANSFORM DATA | → | MULTIPLY BY $\dfrac{-ik}{2\tau}\cos\theta\ \dfrac{e^{ikR}}{R}$ | → | TRANSFORM COORDINATES BY EQ. (4.3) | → |
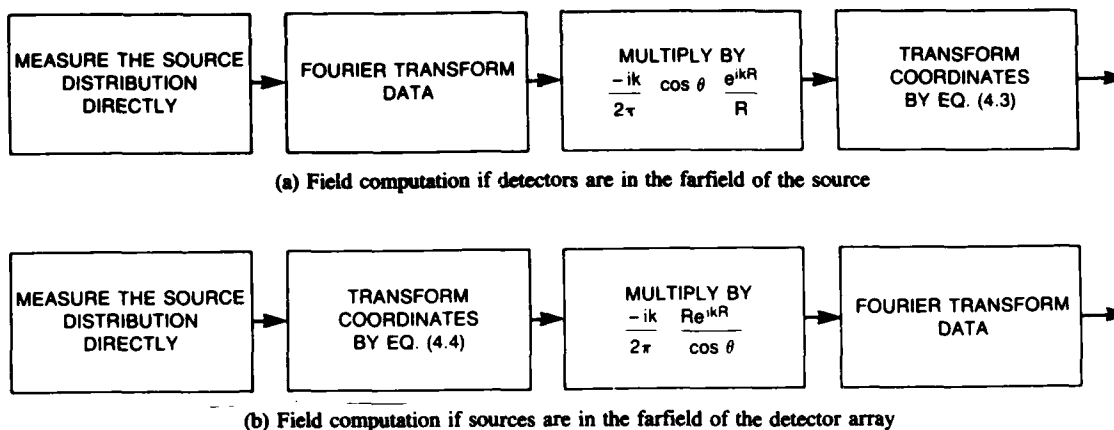
(a) Field computation if detectors are in the farfield of the source

| MEASURE THE SOURCE DISTRIBUTION DIRECTLY | → | TRANSFORM COORDINATES BY EQ. (4.4) | → | MULTIPLY BY $\dfrac{-ik}{2\pi}\ \dfrac{Re^{ikR}}{\cos\theta}$ | → | FOURIER TRANSFORM DATA | → |

(b) Field computation if sources are in the farfield of the detector array

Fig. 5 — Differences in propagation calculations using the Fraunhofer
approximations of the (a) second and (b) third kinds

in Fig. 5 should work. Examination of the nonlinear coordinate transformations given by Eqs. (15) and (16) indicate that in the limit as R gets very large relative to both b and b' we get

$$\xi_x \sim Ds_x,$$

$$\xi_y \sim Ds_y, \tag{17}$$

and

$$s_x \sim \xi_x'/D,$$

$$s_y \sim \xi_y'/D, \tag{18}$$

so that in this limit the transformations represent only a linear scaling. Substitution from Eqs. (17) and (18) into Eqs. (10) and (12) while setting $R = D$ gives

$$\psi(\vec{\xi}') = -ik/2\pi[\exp(ikD)/D]\int\int_{-\infty}^{\infty}\psi(\vec{\xi})[\exp(-ik\vec{\xi}\cdot\vec{\xi}'/D)d\xi_x d\xi_y], \tag{19}$$

for either case which shows that they are identical in this limit.

The Fraunhofer approximations of the second and third kinds have another interesting difference when they are applied to inverse problems. As we discussed, the Fraunhofer approximation of the second kind can be inverted for use in computing the source distribution from measured farfield data, but only to within the resolution limit of a diffraction-limited lens with a numerical aperture of unity. The Fraunhofer approximation of the third kind can also be inverted and applied to inverse problems, but because of the requirement that the detector array be limited to circle of radius where Eq. (11) is satisfied, the field cannot be measured outside of this region. This restriction leads to a different resolution limit on the calculations for the source distribution. In this case the fundamental resolution limit is equivalent to that of a diffraction-limited lens with a numerical aperture of b'/R, which, because of Eq. (11), is much poorer than the best resolution possible when using the Fraunhofer approximation of the second kind.

9

Table 1 summarizes the different properties of the three kinds of Fraunhofer approximations discussed in this section.

Table 1 — Differences Between Fraunhofer Approximations

	First Kind	Second Kind	Third Kind
Source domain	Near origin	$z = 0$ plane	$z \geq 0$ half space
Source dimen.	3-D, linear	2-D, linear	2-D, angular
Det. domain	Far from origin	Far from O, $z \geq 0$	$z = 0$ plane
Det. dimensions	2-D, angular	2-D, angular	2-D, linear
FT domain	Sphere	Plane	Plane
FT dimensions	3-D	2-D	2-D
Large parm.	(Source radius) ^{2}/R	(Aperture dia.) ^{2}/R	(Det. dia.) ^{2}/R

1.5 Conclusions

The Fraunhofer approximation can take at least three forms that are very different and are useful in different applications. The Fraunhofer approximations of the first, second, and third kinds, defined in this section are well known in radiation physics, optics, and electrical engineering, respectively. This appears to be because their different properties best suit them for important applications in these fields. However, each is not as well known outside of its respective field. Since occasionally problems arise in optics that can be best analyzed by a Fraunhofer approximation other than that of the second kind, it would seem useful to be aware of all three of these forms.

2 THREE FRAUNHOFER APPROXIMATIONS FOR THE PROPAGATION OF THE CROSS-SPECTRAL DENSITY FUNCTION

2.1 Introduction

Section 1 (also Ref. 15) shows that at least three different kinds of Fraunhofer approximations in scalar diffraction theory have important differences in both conditions for validity and mathematical structure.

In the next three subsections we apply each of these approximations to coherence theory to describe the propagation of the cross-spectral density function from the sources of the field to detectors far away. As was the case in diffraction theory we find significant differences between the three approximations. In the fourth subsection we show that in two of these approximations the propagation equations can be easily inverted to deal with inverse problems. The inverse propagation equations suggest a method for refocusing a radio telescope to observe objects in the nearfield of its antenna array.

2.2 Fraunhofer Approximation of the First Kind

Consider Fig. 6 that shows a three-dimensional source distribution localized to a region about the origin and radiating an electromagnetic field in all directions. We consider the typical monochromatic, Cartesian components of the field $\psi(x, \omega)$ and the charge-current distribution $\rho(x, \omega)$, which are related by the inhomogeneous Helmholtz equation

$$(\nabla^2 + k^2)\psi(x, \omega) = -4\pi\rho(x, \omega),\tag{20}$$

where ω is the radial frequency and $k = 2\pi/\lambda = \omega/c$.
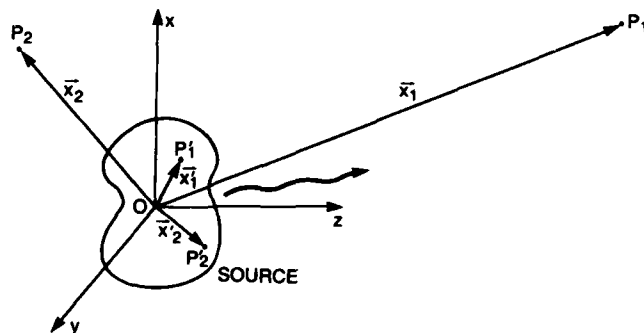
10

Fig. 6 — Configuration for the Fraunhofer
approximation of the first kind

In this section we assume that the source fluctuates in an irregular manner and treat $\psi(\mathbf{x}, \omega)$ and $\rho(\mathbf{x}, \omega)$ (for each frequency ω) as random variables. The second-order statistical properties of these random variables will be characterized in a manner conventional in coherence theory by the cross-spectral density functions W_ρ and W_ψ defined by

$$< \rho(\mathbf{x}_1, \omega)\rho^*(\mathbf{x}_2, \omega') > = W_\rho(\mathbf{x}_1, \mathbf{x}_2, \omega)\delta(\omega - \omega') \tag{21a}$$

and

$$< \psi(\mathbf{x}_1, \omega)\psi^*(\mathbf{x}_2, \omega') > = W_\psi(\mathbf{x}_1, \mathbf{x}_2, \omega)\delta(\omega - \omega'), \tag{21b}$$

which represent the ensemble average of the random variables at two different points $\mathbf{x}_1$ and $\mathbf{x}_2$ and at two different frequencies ω and ω'.

We found in Subsection 1.2 that if the source is completely contained within a sphere of radius a centered on the origin and if the field point is at a distance R from the origin that is outside of the Rayleigh range of the source, i.e.,

$$R >> ka^2, \tag{22}$$

then from Eq. (5) the field amplitude at $\mathbf{x}$ is given as a function of the three-dimensional Fourier transform of the source distribution over the source points $\mathbf{x}'$ by the Fraunhofer approximation of the first kind, viz.,

$$\psi(R\mathbf{s}) = [\exp{(ikR)}/R] \iiint\limits_{-\infty}^{\infty} \rho(\mathbf{x}') \exp{(-ik\mathbf{s} \cdot \mathbf{x}')} d^3\mathbf{x}', \tag{23}$$

where $R = |\mathbf{x}|$ is the distance and $\mathbf{s}$ is a unit vector in the direction from the origin to the field point at $\mathbf{x}$. Upon substitution from Eq. (23) into Eq. (21b) and then by using Eq. (21a) we find that the cross-spectral density function in the farfield of the source is given by

$$W_\psi(R_1\mathbf{s}_1, R_2\mathbf{s}_2) = \{\exp{[ik(R_1 - R_2)]}/R_1R_2\}$$

$$\times \iiint\limits_{-\infty}^{\infty} \iiint\limits_{-\infty}^{\infty} W_\rho(\mathbf{x}_1', \mathbf{x}_2') \exp{[-ik(\mathbf{s}_1 \cdot \mathbf{x}_1' - \mathbf{s}_2 \cdot \mathbf{x}_2')]} d^3\mathbf{x}_1' d^3\mathbf{x}_2', \tag{24}$$

11

where we drop the argument ω from here on (for a similar result see Ref. 2, Eq. (3.3)). Equation (24) is the second-order (in the field amplitude) form of the Fraunhofer approximation of the first kind that gives the field cross-spectral density function in the radiation zone of a three-dimensional source as a double three-dimensional Fourier transform of the cross-spectral density function of the source. In Eq. (24) s_1 and s_2 represent unit vectors from the origin toward the field points at x_1 and x_2, respectively, $R_1 = |x_1|$, $R_2 = |x_2|$, and the two volume integrals are over the source points at x_1' and x_2', as shown in Fig. 6.

Let us now consider the important special case for which the source is quasi-homogeneous [16, Eq. (3.5)] so that

$$W_\rho(x_1', x_2') = I_\rho[(x_1' + x_2')/2]\,\mu(x_1' - x_2'), \tag{25}$$

where I_ρ is a slow function relative to μ. By this we mean that μ is zero outside of some domain in which $|x_1' - x_2'|$ is smaller than some fixed constant d' and I_ρ is constant over any domain where $|x_1' + x_2'|/2$ varies by no more than d' [16, Section 3]. The function $\mu(x_-')$ appearing in Eq. (25) is a normalized correlation coefficient that has a maximum value of unity that always occurs when $|x_-'| = 0$. By substitution from Eq. (25) into Eq. (24) we obtain

$$W_\psi(R_1 s_1, R_2 s_2) = \{\exp[ik(R_1 - R_2)]/R_1 R_2\}\hat{I}_\rho(s_1 - s_2)\,\hat{\mu}[(s_1 + s_2)/2], \tag{26}$$

where the caret indicates three-dimensional Fourier transforms

$$\hat{I}_\rho(\bar{\xi}) = \int\!\!\!\int\!\!\!\int_{-\infty}^{\infty} I_\rho(x_+)\exp(-ikx_+' \cdot \bar{\xi})d^3x_+', \tag{27}$$

and

$$\hat{\mu}(\bar{\xi}) = \int\!\!\!\int\!\!\!\int_{-\infty}^{\infty} \mu(x_-')\exp(-ikx_-' \cdot \bar{\xi})d^3x_-' \tag{28}$$

[16, Eq. (2.3.10)].

Equation (26) is an important result. It applies to the usual thermal sources and to most other nonlaser sources. It leads to a pair of reciprocity theorems that are very important in radiation theory (see Ref. 16, Section 3 for a detailed discussion of these theorems).

2.3 Fraunhofer Approximation of the Second Kind

Assume that the source is a planar, secondary source in the $z = 0$ plane, as shown in Fig. 7, instead of the three-dimensional, primary source distribution discussed in the last subsection, and assume that it radiates only into the $z \geq 0$ half space. We found in Subsection 1.2 that if such a source is completely contained within a circle of radius b about the origin and if the field point is at a distance R from the origin that is outside of the Rayleigh range of the source, i.e.,

$$R >> kb^2, \tag{29}$$

then from Eq. (10) the field in any direction s from the origin into the $z \geq 0$ half space can be given as a function of the two-dimensional Fourier transform over the source distribution by the Fraunhofer approximation of the second kind, viz.,

$$\psi(Rs) = (-ik/2\pi)\cos\theta\,\exp(ikR)/R \int\!\!\!\int_{-\infty}^{\infty} \psi^{(0)}(x')\exp(-iks \cdot x')d^2x', \tag{30}$$
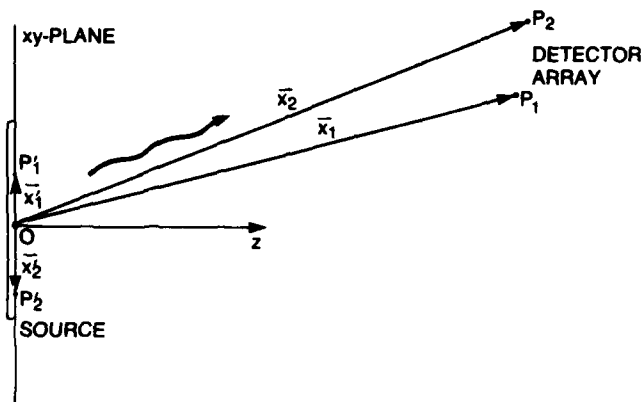
Fig. 7 — Configuration for the Fraunhofer
approximation of the second kind

where θ is the angle that x makes with the $+z$ axis, $R = |x|$, and $s = x/R$. By substitution from Eq. (30) into Eq. (21b) and then by using Eq. (21b) we have

$$W_\psi(R_1 s_1, R_2 s_2) = (k/2\pi)^2 \cos \theta_1 \cos \theta_2 \{\exp [ik(R_1 - R_2)]/R_1 R_2\}$$

$$\times \int\int_{-\infty}^{\infty} \int\int_{-\infty}^{\infty} W_\psi^{(0)}(x_1', x_2') \exp [-ik(s_1 \cdot x_1' - s_2 \cdot x_2')] d^2 x_1' d^2 x_2'. \tag{31}$$

Equation (31) gives the field cross-spectral density function in the radiation zone of the two-dimensional source distribution as a double two-dimensional Fourier transform of the cross-spectral density function of the field between the source positions x_1' and x_2' in the $z = 0$ plane. This is the second-order form of the Fraunhofer approximation of the second kind.

Now we will consider the special case for which the two-dimensional source distribution is quasi-homogeneous, i.e.,

$$W_\psi^{(0)}(x_1', x_2') = I[(x_1' + x_2')/2] \, \mu(x_1' - x_2'), \tag{32}$$

where again I is a slow function relative to μ and μ is a correlation coefficient. Upon substitution from Eq. (32) into Eq. (31) we have

$$W_\psi(R_1 s_1, R_2 s_2) = (k/2\pi)^2 \cos \theta_1 \cos \theta_2 [\exp ik (R_1 - R_2)/R_1 R_2]$$

$$\times \tilde{I}(s_1 - s_2) \tilde{\mu}[(s_1 + s_2)/2], \tag{33}$$

where the tilde represents a two-dimensional Fourier transform

$$\tilde{I}(\bar{\xi}) = \int\int_{-\infty}^{\infty} I(x_+') \exp (-ik x_+' \cdot \bar{\xi}) d^2 x_+', \tag{34}$$

and

$$\tilde{\mu}(\bar{\xi}) = \int\int_{-\infty}^{\infty} \mu(x_-') \exp (-ik x_-' \cdot \bar{\xi}) d^2 x_-'. \tag{35}$$

13

Equation (33) is very important in coherence theory. It applies to thermal as well as most other nonlaser sources. It leads to the van Cittert Zernike theorem as well as to a closely related, reciprocal theorem. This has been discussed in detail elsewhere [17, Section IV].

Equation (31) appears to be mathematically similar in form to Eq. (24) except for two differences. The first difference is that the cross-spectral density function inside of the integral in Eq. (31) is between values of the field amplitude in the source plane rather than values of the source distribution itself. This gives rise to some additional (obliquity) factors appearing in Eq. (31). The second difference is that the Fourier transform in Eq. (31) is two dimensional rather than three dimensional. As we shall see later, this difference in dimensionality has important consequences.

The conditions for validity of Eqs. (24) and (31) are of course quite different. Equation (24) applies to the field outside of the Rayleigh range in any direction from a three-dimensional primary source distribution about the origin. Equation (31) applies to the field outside of the Rayleigh range in the $z \geq 0$ half space of a secondary planar source in the $z = 0$ plane.

2.4 Fraunhofer Approximation of the Third Kind

For the last case, we assume that the detector array, not the source, is distributed over the $z = 0$ plane near the origin as shown in Fig. 8. Then we assume that it is the source of the field that is located in the $z \geq 0$ half space away from the origin. Comparison of Figs. 7 and 8 shows that these two cases are the same except that the positions of the source points and field points have been interchanged. In Subsection 1.3 it is shown that if the detector array is completely contained within a circle of radius b' from the origin and that every point in the source at a distance R from the origin is outside of the Rayleigh range of the detector array, i.e.,

$$R >> kb'^2, \tag{36}$$

then from Eq. (12) the field measured by the detector at x', can be given as the two-dimensional Fourier transform over the source distribution by the Fraunhofer approximation of the third kind, viz.,

$$\psi^{(0)}(\mathbf{x}') = -ik/2\pi \iint_{s_x^2 + s_y^2 \leq 1} [\psi(R\mathbf{s}) \exp(ikR)/R] \exp(-ik\mathbf{s} \cdot \mathbf{x}')R^2(ds_x ds_y/s_z), \tag{37}$$

where $\mathbf{s} = (s_x, s_y, s_z)$ is the unit vector from the origin in the direction of the source point at $\mathbf{x}$. Upon substitution from Eq. (37) into Eq. (21b) and by using Eq. (21a) we find that

$$W_\psi^{(0)}(\mathbf{x}_1', \mathbf{x}_2') = (k/2\pi)^2 \iint_{D_1} \iint_{D_2} \{W_\psi(R_1\mathbf{s}_1, R_2\mathbf{s}_2) \{\exp[ik(R_1 - R_2)]/R_1 R_2\}$$

$$\times \exp[-ik(\mathbf{s}_1 \cdot \mathbf{x}_1' - \mathbf{s}_2 \cdot \mathbf{x}_2')] (R_1^2 ds_{1x} ds_{1y}/s_{1z}) (R_2^2 ds_{2x} ds_{2y}/s_{2z}), \tag{38}$$

where $\mathbf{s}_1 = (s_{1x}, s_{1y}, s_{1z})$ and $\mathbf{s}_2 = (s_{2x}, s_{2y}, s_{2z})$ are the directions from the origin to the source points at $\mathbf{x}_1$ and $\mathbf{x}_2$, $R_1 = |\mathbf{x}_1|$, $R_2 = |\mathbf{x}_2|$, and D_1 and D_2 are the domains of integration where $s_{1x}^2 + s_{1y}^2 \leq 1$ and $s_{2x}^2 + s_{2y}^2 \leq 1$, respectively. Equation (38) gives the field cross-spectral density function between points $\mathbf{x}_1'$ and $\mathbf{x}_2'$ within the detector array in the $z = 0$ plane as a double two-dimensional Fourier transform over the field cross-spectral density function between the source positions at $R_1\mathbf{s}_1$ and $R_2\mathbf{s}_2$. This is the second-order form of the Fraunhofer approximation of the third kind.
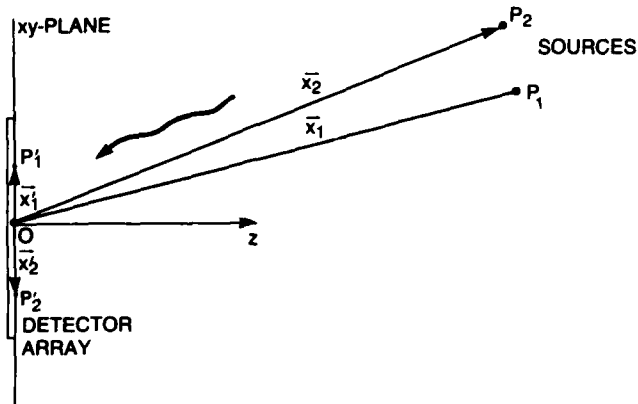
14

Fig. 8 — Configuration for the Fraunhofer
approximation of the third kind

We will consider the special case for which the source distribution is quasi-homogeneous so that

$$W_\psi(\mathbf{x}_1, \mathbf{x}_2) = I[(\mathbf{x}_1 + \mathbf{x}_2)/2]\,\mu(\mathbf{x}_1 - \mathbf{x}_2), \tag{39}$$

where I is again a slow function relative to μ and μ is a correlation coefficient. Then upon substitution from Eq. (39) into Eq. (38) we have

$$W_\psi(\mathbf{x}_1, \mathbf{x}_2) = (k/2\pi)^2 \tilde{G}(\mathbf{x}_1' - \mathbf{x}_2')\,\tilde{\mu}[(\mathbf{x}_1' + \mathbf{x}_2')/2], \tag{40}$$

as shown in Appendix B, where

$$\tilde{G}(\bar{\xi}) = \iint_{2\pi} I(R\mathbf{s}) \exp(-ik\mathbf{s} \cdot \bar{\xi})R^2(ds_x\,ds_y\,/s_z^2) \tag{41}$$

and

$$\tilde{\mu}(\bar{\xi}) = \iint_{-\infty}^{\infty} \mu(R\mathbf{s}_-) \exp(-ik\mathbf{s}_- \cdot \bar{\xi})ds_{-x}\,ds_{-y}. \tag{42}$$

Reference 18, Eq. (2.11) contains a different derivation of Eq. (40) for the special case where the source is completely incoherent.

Equation (40) is different from Eqs. (26) and (33) in that it gives the cross-spectral density function for the field over a detector array if the sources are outside of the Rayleigh range of the detector array. The results in the earlier sections give the cross-spectral density function for detectors outside of the Rayleigh range of the sources, i.e., in the farfield. These are very important differences. Usually if one condition applies the other does not.

There are two formal differences between Eqs. (40) and (33). The first, and most important, difference is in the coordinates. In Eq. (33) the Fourier transformation is from linear coordinates within the source plane at $z = 0$ to angular coordinates from this origin to the field points far away. In Eq. (40) the Fourier transform is from angular coordinates that the source points subtend from an origin within the detector array within the $z = 0$ plane to linear coordinates within the plane of the

15

detector array. This is a very important difference as we shall see when dealing with inverse problems in the next subsection.

The second formal difference between Eqs. (40) and (33) is the additional factors appearing in the kernel of Eq. (41). In general R and s_z are functions of s and cannot be removed from the integral. However, for the special case where the sources are all located on a hemisphere of a constant radius R centered at the origin and the sources are localized within a region that subtends such a small angle from the origin that s_z can be approximated by unity, then Eq. (40) becomes

$$W_\psi(\mathbf{x}_1', \mathbf{x}_2') = (kR/2\pi)^2 \tilde{I}(\mathbf{x}_1' - \mathbf{x}_2') \tilde{\mu}[(\mathbf{x}_1' + \mathbf{x}_2')/2)]. \tag{43}$$

Equation (43) differs from Eq. (33) because of the different conditions required for their validity, the location of the origin of the coordinates, and the different use of linear and angular coordinates.

2.5 Applications of the Fraunhofer Approximations to Inverse Problems

An important example of the application of the Fraunhofer approximations is in their use in inverse problems. In an inverse problem source parameters are calculated from measurements made of the field that they radiate or scatter. Fraunhofer approximations are especially useful in this work since the relationship between source and field parameters appears as easily inverted Fourier transforms. Leaving the more complicated case of the Fraunhofer approximation of the first kind to another study, the intensity distributions describing the sources for the Fraunhofer approximation of the second and third kinds, respectively, are given by inverting Eqs. (33) and (40), as shown in Appendix C, to get the source intensity

$$I(\mathbf{x}') = I_0/\lambda^2 \iint\limits_{-\infty}^{\infty} g_\psi'(\xi,\eta) \exp{(ik\vec{\xi} \cdot \mathbf{x}_1')} d\xi d\eta, \tag{44}$$

if Eq. (29) is valid, or

$$I(R\mathbf{s}) = G_0 (\cos^2\theta/\lambda^2 R^2) \iint\limits_{-\infty}^{\infty} g_\psi(\mathbf{x}_-') \exp{(ik\mathbf{s} \cdot \mathbf{x}_-')} d^2\mathbf{x}_-, \tag{45}$$

if Eq. (36) is valid, where I_0 and G_0 are constants,

$$g_\psi(x_1' - x_2', y_1' - y_2') = W_\psi(\mathbf{x}_1', \mathbf{x}_2')/\sqrt{W_\psi(\mathbf{x}_1', \mathbf{x}_1')W_\psi(\mathbf{x}_2', \mathbf{x}_2')},$$

$$\text{iffi } x_1'^2 + y_1'^2 \le b'^2 \text{ and } x_2'^2 + y_2'^2 \le b'^2,$$

$$= 0 \text{ otherwise} \tag{46}$$

is the normalized correlation coefficient measured with the detector array over the $z = 0$ plane, and

$$g_\psi'(s_{1x} - s_{2x}, s_{1y} - s_{2y}) \triangleq W_\psi(R_1\mathbf{s}_1, R_2\mathbf{s}_2) \exp{[-ik(R_1 - R_2)]}/\sqrt{W_\psi(R_1\mathbf{s}_1, R_1\mathbf{s}_1)W_\psi(R_2\mathbf{s}_2, R_2\mathbf{s}_2)},$$

$$\text{iffi } s_{1x}^2 + s_{1y}^2 \le 1 \text{ and } s_{2x}^2 + s_{2y}^2 \le 1,$$

$$\triangleq 0 \text{ otherwise}, \tag{47}$$

is a normalized, phase-shifted correlation coefficient measured over the detector array away from $z = 0$ plane. In Eqs. (46) and (47) the correlation coefficients are spatially stationary.

Note that the main formal difference between Eqs. (44) and (45) is the different coordinates in the two Fourier conjugate spaces and the obliquity factors. In Eq. (44) the transform is from a space linear with the difference in angle subtended from the origin at the sources by the points at which the field correlation function is measured into a space linear with the source plane coordinates, as shown in Fig. 7. In Eq. (45) the transform is from coordinates linear with the position of the detectors in the $z = 0$ plane into angular coordinates linear with the angle that the source point subtends from the $+z$ axis. Since the transformation from linear to angular coordinates is not a linear transformation (see Eqs. (15) and (16)), this difference is important in the processing of field correlation function data to obtain source intensity.

An important example of this inverse problem is radio astronomy where correlations of the field radiated by astronomical sources are measured by an array of antennas at the surface of Earth and then are used to calculate the secondary source distribution over a hemisphere outside of the Rayleigh range of the array. Equation (45) is the basis for the present radio telescopes that image sources outside of the Rayleigh range of the antenna array [18]. Equation (44) could be used as the basis of a new application of a radio telescope to image a compact source distribution that is within the Rayleigh range of the antenna array but for which the antenna array is in the farfield of the source. However, because of the formal differences between Eqs. (44) and (45) the data from a radio telescope, used to image a small source distribution inside the Rayleigh range of the antenna array, will require different processing to image sources outside of the Rayleigh range of the array. Because the coordinate transformation from linear to angular coordinates, required in Eq. (44) before Fourier transformation, is dependent on $R(x_+)$ (the range from each antenna to the origin within the source distribution), the resulting image will be accurate only for the sources that are near enough to the origin (in agreement with the condition in Eq. (29)). It therefore appears that this transformation of the correlation function data to angular coordinates before the Fourier transformation refocuses the telescope on the localized source distribution and is analogous to focusing a camera on an object that is too close to be in focus when the camera is focused at infinity. This procedure is discussed in Section 3 (see also Ref. 19).

2.6 Differences Between Fraunhofer Approximations

This subsection summarizes and discusses some of the more important differences discovered between the Fraunhofer approximations of the first, second, and third kinds.

A major mathematical difference between the Fraunhofer approximation of the first kind (Eq. (24)) and the others is that it represents a Fourier transform from a six-dimensional space to a four-dimensional space. This is because x_1' and x_2' in Eq. (24) are ordinary vectors with three independent components each, while s_1 and s_2 are unit vectors with only two independent components each. It is therefore not clear that Eq. (24) can be generally inverted to apply to inverse problems. It appears likely, however, that inversion is possible for some special cases. The Fraunhofer approximations of the second and third kind in Eqs. (31) and (38) are not as difficult to invert. Appendix C shows how this can be done for quasi-homogeneous sources when certain approximations are made.

The important differences in the Fraunhofer approximations of the second and third kinds are both in form and in conditions for validity. The difference in conditions for validity were described during derivation. The Fraunhofer approximation of the second kind is valid only if the domain of the source distribution is small enough that the detectors can all be located outside of the Rayleigh range of the source distribution. On the other hand, the Fraunhofer approximation of the third kind is

valid only if the detector array is small enough that the sources can all be placed outside of the Rayleigh range of the detector array. Usually if one approximation applies the other does not. In cases where both approximations apply the formal differences between them can be removed by small angle approximations (see Subsection 1.4).

The formal differences between the Fraunhofer approximations of the second and third kind are twofold, differences in both the coordinate systems and the obliquity factors. It has been pointed out (Eq. (16)) that the coordinate transformations from linear to angular coordinates in Eqs. (38), (41), (43), or (44) needed to prepare the data for Fourier transformation are in general nonlinear transformations and do not commute with the Fourier transformation. No such coordinate transformations are required for Eqs. (24), (26), (31), (33), or (45), for which the transformed data come out automatically in angular coordinates and need to be transformed into linear coordinates only if desired. Thus the formal differences in processing data by using different Fraunhofer approximations is nontrivial (viz, Section 3).

2.7 Conclusions

The differences between Fraunhofer approximations of the first, second, and third kinds, which are discussed in terms of scalar diffraction theory in Section 1, are also found to exist when these theories are extended to describe the propagation of the cross-spectral density function. The Fraunhofer approximation of the third kind leads to the formulas that are usually used in radio astronomy to process the data from a radio telescope to image sources in the farfield of the antenna array. The use of the Fraunhofer approximation of the second kind, instead, leads to modified formulas. It appears that these formulas show how to process these data differently so that the radio telescope is refocused to image objects in the nearfield of the antenna array.

3 REFOCUSING A RADIO TELESCOPE TO IMAGE SOURCES IN THE NEARFIELD OF THE ANTENNA ARRAY

3.1 Introduction

Radio telescopes have been used since the 1950s to image radio sources that are very far from the antenna arrays. There has been some interest at the Naval Research Laboratory in building new radio telescopes with very large space borne antenna arrays to improve resolution. Some of these arrays would be so large that some sources within the solar system would be within their nearfield so that the usual methods for forming images fail. Some experimental work has already been done toward refocusing a radio telescope to look at nearby objects but without the support of any detailed theoretical understanding. This work has been done principally by use of optical analogies.

In the present section a theoretical foundation is provided for understanding the refocusing problem in a more systematic way by use of optical coherence theory. The first subsection describes the operation of a conventional radio telescope focused at infinity. The second subsection extends this theory to describe some methods for refocusing the telescope to image objects that are much closer to the antenna array. This study is based on the formulation derived in Sections 1 and 2 (also see Refs. 15 and 20).

3.2 Conventional Farfield Imaging

Conventionally a radio telescope is used to image radio sources that are in the farfield of the antenna array of the instrument. This is analogous to a camera focused at infinity. If the radiation source is in the farfield of the antenna array, it makes no difference to the adjustment of the telescope

or to the computation of the image just how far the source is from the telescope. All objects are in focus simultaneously if they are in the farfield of the antenna array. It is important to remember that in radio astronomy the term farfield refers to the source being in the farfield of the antenna array. As we shall soon see this is quite different than having the antenna in the farfield of the sources just as discussed in Sections 1 and 2. The conventional method by which a radio telescope images radio sources in its farfield is described in this subsection for comparison to the new technique for refocusing the telescope to image sources in its nearfield.

Consider an antenna array for a radio telescope arranged over the $z = 0$ plane near the origin, as shown in Fig. 9, irradiated by radio waves from sources in its farfield. Since the sources are all in the farfield of the antenna array, to image them we need only calculate the intensity over a hemisphere of radius R from the origin.
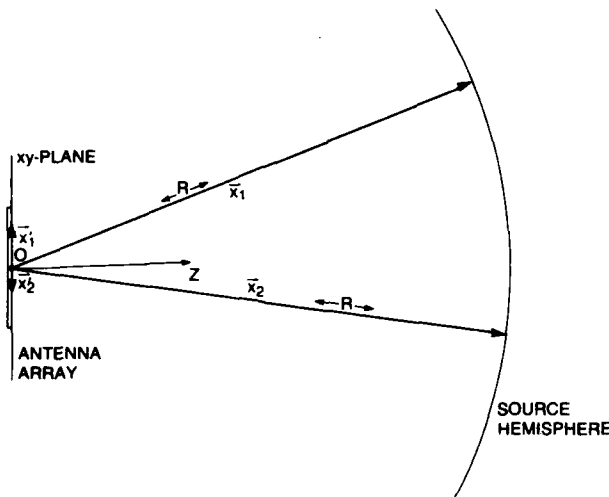

Fig. 9 — Conventional radio telescope focused at infinity

The antennas measure the amplitude of one component of the transverse electric field at points indicated by the position vector x' from the origin as shown in Fig. 9. The signal from each antenna is then processed as shown in Fig. 10. The signals are detected by a receiver, reduced to a convenient IF, and bandlimited to a narrow frequency spectrum. Then the signals are passed through delay lines that point the array toward the source so that the normal to the plane of the antenna array points in the direction of interest. The resulting signals are then multiplied together and the product time averaged to form correlation functions between signals from antenna pairs, viz.,

$$\Gamma(\mathbf{x}_1, \mathbf{x}_2, 0) = \lim_{T \to \infty} 1/2T \int_{-T}^{T} \Psi(\mathbf{x}_1, t) \, \Psi^*(\mathbf{x}_2, t) dt, \tag{48}$$

where $\Psi(\mathbf{x}, t)$ represents the complex field amplitude of the traveling wave propagating from the source to the antenna array, after it has been detected and bandlimited by the telescope.

We represent the second-order statistical properties of the field by use of either the mutual coherence function or the cross-spectral density function of optical coherence theory (for general description see Refs. 3 and 21, and for applications to radio astronomy see Ref. 18). The second-order statistical properties of the field are completely specified by the mutual coherence function

$$\Gamma(\mathbf{x}_1, \mathbf{x}_2, \tau) = \lim_{T \to \infty} 1/2T \int_{-T}^{T} \Psi(\mathbf{x}_1, t + \tau) \, \Psi^*(\mathbf{x}_2, t) dt, \tag{49}$$
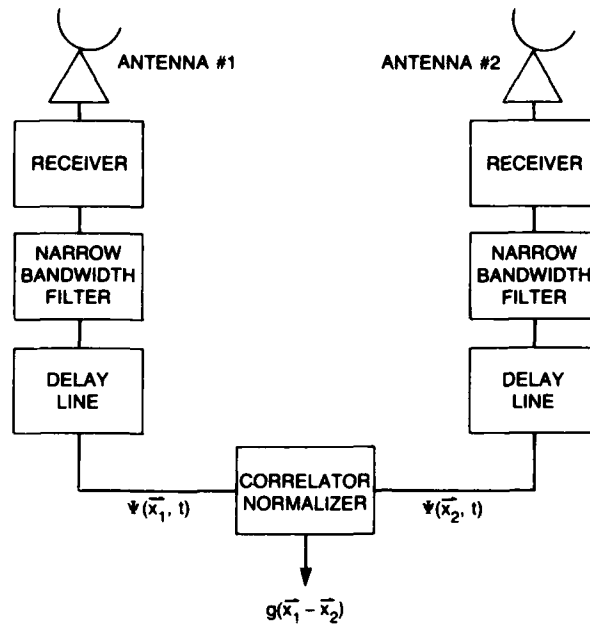
19

Fig. 10 — A typical radio telescope

which is usually defined by using an ensemble average instead of the time average used in radio astronomy. These are equivalent if the statistics of the source are assumed to be ergodic. Note that Eq. (49) is a simple extension of the function described by Eq. (48), which is measured by the radio telescope. The cross-spectral density function is then defined by the equation

$$W_\omega(\mathbf{x}_1, \mathbf{x}_2) = \int_{-\infty}^{\infty} \Gamma(\mathbf{x}_1, \mathbf{x}_2, \tau) \, e^{i\omega\tau} \, d\tau, \tag{50}$$

as the Fourier transform of the mutual coherence function.

The procedure for forming an image depends critically on some important assumptions. First we must assume that the antenna array is bounded so that all antennas are within a circle of radius a from the origin within the $z = 0$ plane. Second, we must assume that all of the sources are in the farfield of the antenna array so that

$$R >> ka^2, \tag{51}$$

where $k = \omega/c$. And third, we assume that the sources of the field are quasi-homogeneous [17]. Then it is well known (see Eq. (45) and the preceding derivation) that the intensity associated with the measured component of the electric field over the hemisphere at infinity (or equivalently at fixed distance R from the origin) is given by the Fourier transform of the normalized cross-spectral density function, i.e.,

$$I(R\mathbf{s}) = G_0 \cos^2 \theta / \lambda^2 R^2 \iint_{-\infty}^{\infty} g(\mathbf{u}) e^{-ik\mathbf{u}\cdot\mathbf{s}} d^2\mathbf{u}, \tag{52}$$

20

where

$$g(x_1' - x_2') \triangleq W_\omega(x_1', x_2')/\sqrt{W_\omega(x_1', x_1')W_\omega(x_2', x_2')},$$

$$\text{iffi } |x_1| \leq a \text{ and } |x_2| \leq a,$$

$$\triangleq 0 \text{ otherwise,} \tag{53}$$

is a spatially stationary correlation coefficient, s is the unit vector pointing from the origin in the direction of an intensity point on the hemisphere, θ is the angle that s makes with the $+x$ axis, $\mathbf{u} = (u, v)$ where

$$u = x_1' - x_2'$$

and

$$v = y_1' - y_2', \tag{54}$$

are difference coordinates between antenna pairs on the $z = 0$ plane, and G_0 is a constant. If some important restrictions are made on the operation of the radio telescope (see Ref. 18, Section II for a detailed discussion), we can approximate the cross-spectral density function in Eq. (52) by the measured correlation function defined by Eq. (48), i.e., we can use

$$g(\mathbf{u}) = \Gamma(x_1', x_2', 0)/ \sqrt{\Gamma(x_1', x_1', 0)\, \Gamma(x_2', x_2', 0)}$$

$$\text{iffi } |x_1'| \leq a \text{ and } |x_2'| \leq a,$$

$$= 0 \text{ otherwise,} \tag{55}$$

in the kernel of Eq. (52), as shown in Appendix D. Therefore, the image may be obtained by using Eq. (52) by normalizing the data and then performing a Fourier transform from the two-dimensional uv plane of antenna position differences to the two-dimensional angular space given by

$$s_x = x/R$$

and

$$s_y = y/R, \tag{56}$$

where x is a position vector from the origin to a point on the hemisphere as shown in Fig. 9.

If the sources are nearer to the antennas so that they are not in the farfield of the array, then, under some circumstances, there is still a way to refocus the telescope to image these sources.

3.3 Nearfield Imaging

Consider Fig. 11, which shows a localized, planar, secondary, quasi-homogeneous source distribution over the $z = 0$ plane radiating radio waves toward an antenna array of a radio telescope that is located in the $z = D$ plane.
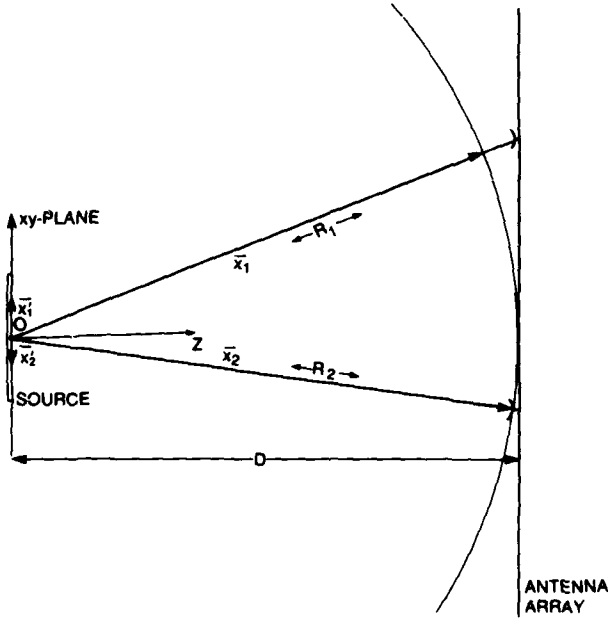
Fig. 11 — Radio telescope focused on a localized source in the nearfield

We assume that the sources are not in the farfield of the antenna array so the D is too small to satisfy Eq. (51). Even so a method exists to form an image by using the same radio telescope described schematically in Fig. 10 but slightly modifying the processing procedure to refocus the telescope onto the nearby sources.

This process requires some important assumptions. First, we assume that the sources are bounded so that they are all contained within a circle of radius b from the origin in the $z = 0$ plane. Second we assume that the antenna array is in the farfield of the sources (it is the other way around for conventional farfield imaging) so that

$$R >> kb^2. \tag{57}$$

Then as shown in Eq. (44), the intensity over the $z = 0$ plane is given by

$$I(\mathbf{x}') \triangleq I_0/\lambda^2 \iint\limits_{-\infty}^{\infty} g'(\vec{\xi}) \exp(ik\mathbf{x}' \cdot \vec{\xi}) d^2\xi, \tag{58}$$

where

$$g'(\mathbf{x}_1/R_1 - \mathbf{x}_2/R_2) \triangleq W_\omega(\mathbf{x}_1', \mathbf{x}_2') \exp[-ik(R_1 - R_2)]/\sqrt{W_\omega(\mathbf{x}_1', \mathbf{x}_1') W_\omega(\mathbf{x}_2', \mathbf{x}_2')},$$

$$\text{iffi } |\mathbf{x}_1|/R \leq 1 \text{ and } |\mathbf{x}_2|/R \leq 1,$$

$$\triangleq 0 \text{ otherwise}, \tag{59}$$

must be calculated from the experimental correlation data.

22

Inspection of Eqs. (58) and (59) suggests a straightforward computational method for refocusing the telescope to image nearby objects. As shown in Appendix E, under almost the same conditions used with the telescope focused at infinity, the correlation coefficient in Eq. (59) can be approximated by

$$g'(\mathbf{x}_1/R_1, \mathbf{x}_2/R_2) = \Gamma(\mathbf{x}_1, \mathbf{x}_2, 0) \exp\left[-ik(R_1 - R_2)\right]/\sqrt{\Gamma(\mathbf{x}_1, \mathbf{x}_1, 0)\Gamma(\mathbf{x}_2, \mathbf{x}_2, 0)},$$

$$\text{iffi } x_1^2 + y_1^2 \leq R_1^2 \text{ and } x_2^2 + y_2^2 \leq R_2^2,$$

$$= 0 \text{ otherwise}, \tag{60}$$

by using the measured correlation function in Eq. (48). Then to form an image of the fields over the hemisphere, g' must be transformed from linear u,v coordinates within the antenna plane to the new, angular coordinates given by

$$\xi = x_1/\sqrt{x_1^2 + y_1^2 + D^2} - x_2/\sqrt{x_2^2 + y_2^2 + D^2},$$

$$\eta = y_1/\sqrt{x_1^2 + y_1^2 + D^2} - y_2^2/\sqrt{x_2^2 + y_2^2 + D^2}, \tag{61}$$

and then Fourier transformed. Equation (61) is a nonlinear coordinate transformation that has a non-trivial effect on the data after Fourier transformation.

Inspection of Eqs. (58) and (59) suggests that it might perhaps be useful to refocus the telescope electronically. This could be done by adjusting the delay lines in Fig. 10 so that the antenna array is electronically moved from the plane to a hemisphere of radius R from the origin as shown in Fig. 11. This can be done since the antennas are in the farfield of the sources and the farfield amplitude is constant along any direction from the origin except for a $1/R$ decay and the usual $\exp(ikR)$ phase shift. This use of the delay lines has the effect of refocusing the antenna array onto the sources in analogy to a refocusing a camera on a nearby object. With refocusing the function in Eq. (59) becomes the same normalized correlation coefficient given in Eq. (53) and it can be calculated from the measured correlation function by using Eq. (55) just as for the case when the telescope was focused at infinity.

If we adjust the delay lines as suggested so that in Eq. (58) $R_1 = R_2 = D$ a constant, then Eq. (61) reduces to

$$\xi = u/D$$

and

$$\eta = v/D, \tag{62}$$

so that Eq. (58) becomes

$$I(\mathbf{x}') = I_0/\lambda^2 D^2 \iint\limits_{-\infty}^{\infty} g(\mathbf{u}) \exp(ik\mathbf{x}' \cdot \mathbf{u}/D^2) du\, dv, \tag{63}$$

23

which is essentially the same as Eq. (52) except for the trivial cos θ factor and the fact that the u,v coordinates in Eq. (63) correspond to the antenna position differences after they are projected onto the hemisphere, not those on the actual physical antenna plane. As shown in Appendix E, the correlation coefficient in the kernel can be approximated by using the measured correlation function as given by Eq. (60) but with exp $(-ik(R_1 - R_2)) = 1$. Thus the data can be processed essentially as before when the telescope was focused at infinity.

In appears clear from these results that we have to either refocus the telescope physically by use of the phase shifters or refocus it mathematically by use of a modified data-processing procedure. In either case we should be able to form an image of the nearby object in a similar manner to an object in the farfield.

3.4 Conclusions

It appears possible to refocus a radio telescope to image radio sources within the nearfield of the antenna array if the antenna array is in the farfield of the source distribution. This is done by refocusing the telescope onto the sources in analogy to a photographic camera. Refocusing can be done either electronically by curving the antenna array into a portion of a hemisphere with a center at the source, or by processing the correlation function data obtained from the antennas in a somewhat modified manner. Neither of these techniques would require any modification to most existing telescopes. The modifications to the data-processing software should not be extensive.

REFERENCES

1. J. D. Jackson, *Classical Electrodynamics* (Wiley, New York, 1962).

2. W. H. Carter and E. Wolf, "Correlation Theory of Wavefields Generated by Fluctuating Three-dimensional, Primary, Scalar Sources I. General Theory," *Optical Acta* **28**, 227-244 (1981).

3. M. Born and E. Wolf, *Principles of Optics*, 5th ed. (Pergamon Press, New York, 1975).

4. J. W. Goodman, *Introduction to Fourier Optics* (McGraw-Hill, New York, 1968).

5. J. D. Kraus, *Antennas* (McGraw-Hill, New York, 1950).

6. A. J. Devaney and E. Wolf, "Radiating and Nonradiating Classical Current Distributions and the Fields They Generate," *Phys. Rev. D* **D8**, 1044-1047 (1973).

7. A. J. Devaney and E. Wolf, "Multipole Expansions and Plane Wave Representations of the Electromagnetic Field," *J. Math. Phys.* **15**, 234-244 (1974).

8. A. T. Friberg, "On the Question of the Existence of Nonradiating Primary Planar Sources of Finite Extent," *J. Opt. Soc. Am.* **68**, 1281-1283 (1978).

9. A. J. Devaney and E. Wolf, "Non-radiating Scalar Sources," in *Coherence and Quantum Optics*, L. Mandel and E. Wolf, eds. (Plenum Press, New York, 1984).

10. K. Kim and E. Wolf, "Non-radiating Monochromatic Sources and Their Fields," *Opt. Commun.* **59**, 1-6 (1986).

11. E. Wolf and M. Nieto-Vesperinas, "Analyticity of the Angular Spectrum Amplitude of Scattered Fields and Some of its Consequences," *J. Opt. Soc. Am.* **A2**, 886-889 (1985).

12. E. Wolf and R. P. Porter, "On the Physical Contents of Some Integral Equations for Inverse Scattering from Inhomogeneous Objects," *Radio Sci.* **21**, 627-634 (1986).

13. E. Wolf, "Three-dimensional Structure Determination of Semitransparent Objects from Holographic Data," *Opt. Commun.* **1**, 153-156 (1969).

14. W. H. Carter, "Inverse Scattering in the First Born Approximation," *Opt. Eng.* **23**, 204-209 (1984).

15. W. H. Carter, "Three Different Kinds of Fraunhofer Approximations: I. Propagation of the Field Amplitude," *Radio Sci.* **23** (publication pending, Nov-Dec, 1988).

16. W. H. Carter and E. Wolf, "Correlation Theory of Wavefields Generated by Fluctuating, Three-dimensional, Primary, Scalar Sources: II. Radiation From Isotropic Model Sources," *Opt. Acta* **28**, 245-259 (1981).

17. W. H. Carter and E. Wolf, "Coherence Theory with Quasihomogeneous Planar Sources," *J. Opt. Soc. Am.* **67**, 785-796 (1977).

18. W. H. Carter and L. E. Somers, "Coherence Theory of a Radio Telescope," *IEEE Trans. Antennas Propag.* **AP-24**, 815-819 (1976).

19. W.H. Carter, "On Refocusing a Radio Telescope to Image Sources in the Near Field of Antenna Array," *IEEE Trans* (publication pending, Mar or Apr, 1989).

20. W. H. Carter, "Three Different Kinds of Fraunhofer Approximations: II. Propagation of the Cross-spectral Density Function," *Radio Sci.* (submitted).

21. J. Perina, *Coherence of Light* (D. Reidel, Boston, 1985).

Appendix A

RECIPROCITY THEOREM

The reciprocity theorem used in antenna theory treats antennas as circuit elements and usually relates only the input and output currents and voltages for coupled antennas. Some work has been done to obtain reciprocity theorems for electromagnetic fields [A1, Chapter 9] but this work is difficult to relate to field propagation as discussed here. Therefore, a generalized field reciprocity theorem is derived in this appendix in the form needed to obtain Eq. (12) from Eq. (10).

First, consider the outgoing field in Fig. 2. Assume that the field arises from primary sources in the $z < 0$ half space and propagates to the right into the $z \geq 0$ half space. Let the $z \geq 0$ half space contain only a homogeneous, isotropic, source-free medium. We also assume that the sources are far enough from the $z = 0$ plane that the effects of evanescent plane waves on the fields in the $z > 0$ half space can be neglected. Then we can always expand the scalar amplitude of the field in this half space into an angular spectrum of homogeneous plane waves in the form

$$\psi_1(\mathbf{x}_2) = \iint_{p_2^2 + q_2^2 \leq 1} A_1(p_2, q_2) \exp[ik(p_2 x_2 + q_2 y_2 + m_2 z_2)]dp_2 dq_2, \tag{A1}$$

where

$$m_2 = \sqrt{1 - p_2^2 - q_2^2}, \quad p_2^2 + q_2^2 \leq 1. \tag{A2}$$

The angular spectrum is found by taking the Fourier transform of Eq. (A1) after setting $z = 0$ to get

$$A_1(p_2, q_2) = 1/\lambda^2 \iint_{-\infty}^{\infty} \psi_1^{(0)}(\mathbf{x}_2') \exp[-ik(p_2 x_2' + q_2 y_2')]dx_2' dy_2', \tag{A3}$$

and the field over the hemisphere of radius R from the origin is found by integrating Eq. (A1) by use of the method of stationary phase to get

$$\psi_1^{(\infty)}(\mathbf{x}_2) \sim -i\lambda z_2/R \, A_1(x_2/R, y_2/R)e^{ikR}/R, \tag{A4}$$

asymptotically as kR becomes large.

Next consider the reciprocal field illustrated in Fig. 3. Assume that this field arises from primary sources to the right of the hemisphere in Fig. 3 and propagates to the left toward the $z = 0$ plane. We assume that the region to the left of the hemisphere contains only a homogeneous, isotropic, source-free medium. We also assume that the primary sources are far enough away from the hemisphere that we can neglect the effects of evanescent plane waves on the field to the left of the hemisphere. Then over the region between the $z = 0$ plane and the hemisphere we can always expand the scalar amplitude of the field into an angular spectrum of homogeneous plane waves in the form

$$\psi_2(\mathbf{x}_3) = \iint_{p_3^2 + q_3^2 \leq 1} A_2(p_3, q_3) \exp[ik(p_3 x_3 + q_3 y_3 - m_3 z_3)]dp_3 dq_3, \tag{A5}$$

27

where

$$m_3 = \sqrt{1 - p_3^2 + q_3^2}, \quad p_3^2 + q_3^2 \leq 1. \tag{A6}$$

The angular spectrum is obtained from Eq. (A5) as

$$A_2(p_3, q_3) = 1/\lambda^2 \iint\limits_{-\infty}^{\infty} \psi_2^{(0)}(x_3') \exp\left[-ik(p_3 x_3' + q_3 y_3')\right] dx_3' dy_3' \tag{A7}$$

and the secondary source distribution over the hemisphere is found from Eq. (A5) to be

$$\psi_2^{(\infty)}(\mathbf{x}_3) \sim i\lambda z_3/R \, A_2(-x_3/R, -y_3/R)e^{-ikR}/R, \tag{A8}$$

asymptotically as kR becomes large.

Let the outgoing field in Fig. 2 be called field one and the incoming field in Fig. 3 be called field two. We assume that field one has an arbitrary secondary source distribution given by

$$\psi_1^{(0)}(\mathbf{x}_2') \triangleq G(\mathbf{x}_2'), \tag{A9}$$

over the $z = 0$ plane. Then by substitution from Eq. (A9) into Eq. (A3) we obtain the angular spectrum

$$A_1(p_2, q_2) = \hat{G}(p_2, q_2) = 1/\lambda^2 \iint\limits_{-\infty}^{\infty} G(x_2') \exp\left[-ik(p_2 x_2' + q_2 y_2')\right] dx_2' dy_2'. \tag{A10}$$

By substitution from Eq. (A10) into Eq. (A4) we find the field distribution over the hemisphere to be

$$\psi_1^{(\infty)}(\mathbf{x}_2) \sim -i\lambda z_2/R \, \hat{G}(x_2/R, y_2/R)e^{ikR}/R. \tag{A11}$$

We now define field two in Fig. 3 to be the reciprocal of field one by requiring that the secondary source distribution over the hemisphere in Fig. 3 be the complex conjugate of the field distribution given in Eq. (A11) for field one over the identical hemisphere in Fig. 2, i.e.,

$$\psi_2^{(\infty)}(\mathbf{x}_3) \triangleq [\psi_1^{(\infty)}(\mathbf{x}_3)]^* = i\lambda z_3/R \, \hat{G}^*(x_3/R, y_3/R)e^{-ikR}/R. \tag{A12}$$

By comparing Eq. (A12) with Eq. (A8) it is clear that field two must have the angular spectrum

$$A_2(p_3, q_3) = \hat{G}^*(-p_3, -q_3). \tag{A13}$$

Upon substituting from Eq. (A10) into Eq. (A1) we find that

$$\psi_1(\mathbf{x}_2) = \iint\limits_{p_2^2 + q_2^2 \leq 1} \hat{G}(p_2, q_2) \exp\left[ik(p_2 x_2 + q_2 y_2 + m_2 z_2)\right] dp_2 dq_2, \tag{A14}$$

28

and then by substituting from Eq. (A13) into Eq. (A5), taking the complex conjugate, setting $p_3 = -p_3$ and $q_3 = -q_3$, we find that

$$\psi_2^*(\mathbf{x}_3) = \iint\limits_{p_3^2 + q_3^2 \leq 1} \hat{G}(p_3, q_3) \exp\left[ik(p_3 x_3 + q_3 y_3 + m_3 z_3)\right]dp_3 dq_3. \tag{A15}$$

By comparing Eqs. (A14) and (A15) it is obvious that at equivalent points in the two spaces, where $\mathbf{x}_2 = \mathbf{x}_3 = \mathbf{x}$, the fields take on values that are complex conjugate to each other so that

$$\psi_1(\mathbf{x}) = \psi_2^*(\mathbf{x}). \tag{A16}$$

Thus if we derive a forward propagation integral for field one in the form

$$\psi_1(\mathbf{x}'') = \iint\limits_{-\infty}^{\infty} \psi_1(\mathbf{x}')h(\mathbf{x}'', \mathbf{x}')d^2\mathbf{x}', \tag{A17}$$

from any plane $z = z'$ to any later field point x'', both contained within the region between the $z = 0$ plane and hemisphere in Fig. 2, then by substitution from Eq. (A16) into Eq. (A17) and taking the complex conjugate we have

$$\psi_2(\mathbf{x}'') = \iint\limits_{-\infty}^{\infty} \psi_2(\mathbf{x}')h^*(\mathbf{x}'', \mathbf{x}')d^2\mathbf{x}', \tag{A18}$$

for the inverse propagator for field two from the corresponding $z = z'$ plane back to the earlier field point at $\mathbf{x}''$.

Thus we have proved a useful reciprocity theorem that can be summarized as follows: If two electromagnetic fields, propagating in opposite directions, taken one at a time, within a source-free, isotropic, and homogeneous medium, are composed only of homogeneous plane waves such that their angular spectra are related by

$$A_1(p, q) \triangleq A_2^*(-p, -q),$$

then they are reciprocal so that the forward propagator for one field (i.e., the kernel h in Eq. (A17)) is the complex conjugate of the inverse propagator (i.e., the kernel h^* in Eq. (A18)) for the other field.

REFERENCE

A1. G.D. Monteath, *Applications of the Electromagnetic Reciprocity Theorem* (Pergamon Press, New York, 1973).

Appendix B
DERIVATION OF EQUATION (40)

Substituting from Eq. (39) into Eq. (38) and transforming variables by using

$$s_- = s_1 - s_2, \qquad s_+ = (s_1 + s_2)/2,$$

$$s_1 = s_+ + s_-/2, \qquad s_2 = s_+ - s_-/2, \tag{B1}$$

and

$$x'_- = x'_1 - x'_2, \qquad x'_+ = (x'_1 + x'_2)/2,$$

$$x'_1 = x'_+ + x'_-/2, \qquad x'_2 = x'_+ - x'_-/2, \tag{B2}$$

then defining R_+ and R_- such that

$$x_1 = R_1 s_1 = R_+ s_+ + R_- s_-/2,$$

$$x_2 = R_2 s_2 = R_+ s_+ - R_- s_-/2, \tag{B3}$$

we obtain

$$W_\psi(x'_1, x'_2) = (k/2\pi)^2 \iint_{-\infty}^{\infty} \iint_{-\infty}^{\infty} \{I(R_+ s_+)\mu(R_- s_-) [\exp [ik(R_1 - R_2)]]\}$$

$$\times \exp [-ik(s_+ \cdot x'_- + s_- \cdot x'_+)](R_1 R_2 ds_{+x} ds_{+y}/s_{1z} s_{2z}) ds_{-x} ds_{-y}. \tag{B4}$$

We must assume that $I(x_+) = 0$ outside of the domains where s_1 and s_2 point into the $z \geq 0$ half space so that we can extend the bounds of integration in Eq. (38) to infinity before we transform coordinates to get Eq. (B4).

We now make use again of our previous assumption that $\mu(x_-) = 0$ outside of the domain where $|x_-| \leq d$. First, we can assume that d is small enough that $R_1(x_1)$, $R_2(x_2)$, s_{1z} and s_{2z}, like $I(x_+)$, do not vary appreciably over the domains where x_1 and x_2 vary by d, so that we have the relations

$$R_1 \approx R_+ \triangleq R,$$

$$R_2 \approx R_+ \triangleq R,$$

31

and

$$s_{1z} \approx s_{2z} \triangleq s_z, \tag{B5}$$

where the geometrical significance of these parameters are shown in Fig. B1. Second, we assume that because of the small d, the angle between s_1 and s_2 in Fig. B1 is small enough, for all values of $x_1 - x_2$ for which the kernel of the integral in Eq. (B4) does not vanish, that we can treat s_+ as a unit vector s.
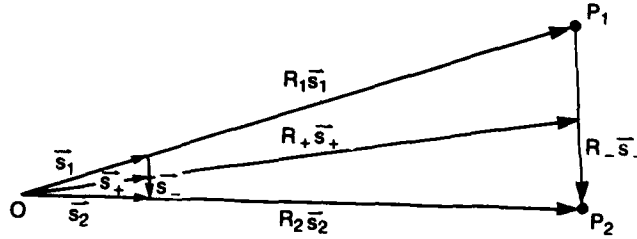

. Fig. B1 — Coordinate transformation in Eq. (44)

By substituting from Eq. (B5) into Eq. (B4) and separating the independent integrations we find that

$$W_\psi(x_1', x_2') = (k/2\pi)^2 \iint\limits_{-\infty}^{\infty} I(Rs) \exp(-iks \cdot x_-') R^2 (ds_x ds_y / s_z^2)$$

$$\times \iint\limits_{-\infty}^{\infty} \mu(R_- s_-) \exp(-iks_- \cdot x_+') ds_{-x} ds_{-y}. \tag{B6}$$

Now, since $I(Rs) = 0$ outside of the domain where $(s_x^2 + s_y^2) \leq 1$, we can reset the range of integration over s so that Eq. (B6) becomes the same as Eq. (40) with the two-dimensional Fourier transforms defined as given by Eqs. (41) and (42).

Appendix C

DERIVATION OF EQUATIONS (44) AND (45)

To derive Eq. (45) from Eqs. (40) and (41) we first normalize the correlation function in Eq. (40) to form the correlation coefficient defined by

$$\mu_\psi(\mathbf{x}_1', \mathbf{x}_2') \triangleq W_\psi(\mathbf{x}_1', \mathbf{x}_2')/\sqrt{W_\psi(\mathbf{x}_1', \mathbf{x}_1')W_\psi(\mathbf{x}_2', \mathbf{x}_2')}, \tag{C1}$$

to obtain

$$\mu_\psi(\mathbf{x}_1', \mathbf{x}_2') = \tilde{G}(\mathbf{x}_1' - \mathbf{x}_2')\tilde{\mu}[(\mathbf{x}_1' + \mathbf{x}_2')/2]/ \left[\tilde{G}(0) \sqrt{\tilde{\mu}(\mathbf{x}_1')\tilde{\mu}(\mathbf{x}_2')} \right]. \tag{C2}$$

Since $I(\mathbf{x}_+)$ in Eq. (39) (as well as R_1, R_2, s_{1z}, and s_{2z}) is a slow function relative to $\mu(\mathbf{x}_-)$, we know from Fourier theory that $\tilde{\mu}(\mathbf{x}_+')$ is a slow function relative to $\tilde{G}(\mathbf{x}_-')$ in Eq. (40). Thus we can assume that $\tilde{G}(x_1' - x_2') = 0$ except over some domain where $|\mathbf{x}_1' - \mathbf{x}_2'| \leq d'$, and that within any domain where $\mathbf{x}_1'$ and $\mathbf{x}_2'$ differ by no more than d' we have

$$\tilde{\mu}(\mathbf{x}_1') \approx \tilde{\mu}(\mathbf{x}_2') \approx \tilde{\mu}[(\mathbf{x}_1' + \mathbf{x}_2')/2], \tag{C3}$$

so that, upon substitution from Eq. (C3) into Eq. (C2) we have

$$\mu_\psi(\mathbf{x}_1', \mathbf{x}_2') \triangleq g_\psi(\mathbf{x}_1' - \mathbf{x}_2') = \tilde{G}(\mathbf{x}_1' - \mathbf{x}_2')/G_0, \tag{C4}$$

where $G_0 = \tilde{G}(0)$ is a constant.

Since the source distribution is defined physically only for points in directions from the origin to the $z \geq 0$ half space we can define $I(Rs)$ in Eq. (41) to have a value of zero for $(s_x^2 + s_y^2) > 1$. Thus we can define the Fourier inverse of Eq. (41) in the usual way. Upon substitution from Eq. (C4) into this inverse, we obtain Eq. (45).

The derivation of Eq. (44) proceeds in a similar manner. Upon substitution from Eq. (33) into Eq. (C1) we have

$$\mu_\psi(R_1\mathbf{s}_1, R_2\mathbf{s}_2) = \tilde{I}(\mathbf{s}_1 - \mathbf{s}_2) \tilde{\mu}[(\mathbf{s}_1 + \mathbf{s}_2)/2] \exp[ik(R_1 - R_2)/ \left[\tilde{I}(0) \sqrt{\tilde{\mu}(\mathbf{s}_1)\tilde{\mu}(\mathbf{s}_2)} \right]. \tag{C5}$$

Because $\tilde{\mu}$ is a slow function relative to $\tilde{I}$ we have

$$\tilde{\mu}(\mathbf{s}_1) \approx \tilde{\mu}(\mathbf{s}_2) \approx \tilde{\mu}[(\mathbf{s}_1 + \mathbf{s}_2)/2], \tag{C6}$$

within the domain where $|\mathbf{s}_1 - \mathbf{s}_2| \leq d/R$, so that Eq. (C5) becomes

$$\mu_\psi(R_1\mathbf{s}_1, R_2\mathbf{s}_2) = \tilde{I}(\mathbf{s}_1 - \mathbf{s}_2)/I_0 \exp[ik(R_1 - R_2)], \tag{C7}$$

where $I_0 = \tilde{I}(0)$ is a constant.

33

Equation (C7) has physical meaning only for unit vectors s_1, and s_2, that point from the origin to the $z \geq 0$ half space; therefore, if we define

$$g'_\psi(s_{1x} - s_{2x}, s_{1y} - s_{2y}) \triangleq \mu_\psi(R_1 s_1, R_2 s_2) \exp[-ik(R_1 - R_2)],$$

$$\text{iffi} \quad s_{1x}^2 + s_{1y}^2 \leq 1 \text{ and } s_{2x}^2 + s_{2y}^2 \leq 1,$$

$$= 0 \text{ otherwise}, \tag{C8}$$

substitute Eq. (C8) into Eq. (C7), solve for $\tilde{I}$, and then substitute the result into the Fourier inverse of Eq. (34) we obtain Eq. (44).

Appendix D

CALCULATION LEADING TO EQUATION (55)

The cross-spectral density function over the antenna plane in Fig. 9 is given by

$$W_\omega^{(0)}(\mathbf{x}_1', \mathbf{x}_2') = (k/2\pi)^2 \hat{G}^{(\infty)}(\mathbf{x}_1' - \mathbf{x}_2', \omega)\hat{\mu}^{(\infty)}[(\mathbf{x}_1' + \mathbf{x}_2')/2, \omega], \tag{D1}$$

where

$$\hat{G}^{(\infty)}(\mathbf{x}_-', \omega) \triangleq \iint_{s_x^2+s_y^2 \leq 1} R^2 I^{(\infty)}(R\mathbf{s})/\cos^2\theta \, \exp\,(ik\mathbf{s} \cdot \mathbf{x}_-')ds_x ds_y, \tag{D2}$$

and

$$\hat{\mu}^{(\infty)}(\mathbf{x}_+', \omega) \triangleq \iint_{-\infty}^{\infty} \mu^{(\infty)}(R\mathbf{s}) \exp\,(ik\mathbf{s} \cdot \mathbf{x}_+')ds_x ds_y \tag{D3}$$

(see Eqs. (40), (41), and (42)), $I^{(\infty)}(\mathbf{x})$ is the intensity distribution over the hemisphere in Fig. 9, and $\hat{\mu}^{(\infty)}(\mathbf{x}_-)$ is the complex degree of spectral coherence over the hemisphere. The field over the hemisphere is assumed to be quasi-homogeneous so that $I^{(\infty)}(\mathbf{x})$ is a slow function relative to $\mu^{(\infty)}(\mathbf{x}_-)$, i.e., $\mu^{(\infty)}(\mathbf{x}_1 - \mathbf{x}_2) = 0$ except within the domain where $|\mathbf{x}_1 - \mathbf{x}_2| \leq d$, and $I^{(\infty)}((\mathbf{x}_1 + \mathbf{x}_2)/2)$ is essentially constant over any domain in which $|(\mathbf{x}_1 + \mathbf{x}_2)|/2$ changes by no more than d.

Upon substitution from Eq. (D1) into the Fourier inverse of Eq. (50) we find that

$$\Gamma^{(0)}(\mathbf{x}_1', \mathbf{x}_2', \tau) = 1/(2\pi) \int_{-\infty}^{\infty} [(k/2\pi)^2 \hat{G}^{(\infty)}(\mathbf{x}_1' - \mathbf{x}_2', \omega)$$

$$\times \hat{\mu}^{(\infty)}[(\mathbf{x}_1' + \mathbf{x}_2')/2, \omega]e^{-i\omega\tau}d\omega. \tag{D4}$$

The signals received by the antennas are filtered so that only those radio waves with frequency ω within a narrow bandwidth $\Delta\omega$ centered on a median frequency contribute to the data. Thus upon transforming Eq. (D4) by setting $\omega = \omega' + \bar{\omega}$ we have

$$\Gamma^{(0)}(\mathbf{x}_1', \mathbf{x}_2', \tau) = e^{-i\bar{\omega}\tau}/(2\pi)^3 \int_{-\Delta\omega}^{\Delta\omega} \hat{G}^{(\infty)}(\mathbf{x}_1' - \mathbf{x}_2', \omega' + \bar{\omega})$$

$$\times \hat{\mu}^{(\infty)}[(\mathbf{x}_1' + \mathbf{x}_2')/2, \omega' + \bar{\omega}] [(\omega' + \bar{\omega})/c]e^{-i\omega'\tau}d\omega'. \tag{D5}$$

Next we make the quasi-monochromatic approximation

$$\Delta\omega \ll \bar{\omega}, \tag{D6}$$

35

so that $\omega' \ll \bar{\omega}$ over the range of integration in Eq. (D5). We can set $(\omega' + \bar{\omega})/c = \bar{\omega}/c = \bar{k}$ where the left-hand side of this expression does not appear in an exponent in Eq. (D5). Now consider

$$\hat{G}^{(\infty)}(x_1' + x_2', \omega' + \bar{\omega}) =$$

$$\iint_{-\infty}^{\infty} [R^2 I^{(\infty)} (Rs)/\cos^2 \theta] \exp \{i[(\omega' + \bar{\omega})/c] \, s \cdot (x_1' - x_2')\}d^2s. \tag{D7}$$

If we restrict the size of the antenna so that

$$|x_1' - x_2'| \ll (2\pi c/\Delta \omega), \tag{D8}$$

then we may neglect the effect of ω' in Eq. (D7) so that, if we assume that $I^{(\infty)}(x)$ is independent of ω', and we can write Eq. (D5) as

$$\Gamma^{(0)}(x_1', x_2', \tau) = (\bar{k}/2\pi)^2 \hat{G}^{(\infty)}(x_1' - x_2', \bar{\omega})\hat{\mu}^{(\infty)}[(x_1' + x_2')/2, \tau] \exp(-i\bar{\omega}\tau), \tag{D9}$$

where

$$\hat{\mu}^{(\infty)}(x_+', \tau) \triangleq (1/2\pi) \int_{-\infty}^{\infty} \hat{\mu}^{(\infty)}(x_+', \bar{\omega} + \omega')e^{-i\omega'\tau}d\omega'. \tag{D10}$$

To eliminate the effects of partial coherence of the source on the data we normalize the mutual coherence function in the usual way to obtain the complex degree of spatial coherence

$$\gamma_\omega^{(0)}(x_1', x_2', \tau) \triangleq \Gamma^{(0)}(x_1', x_2', \tau)/\sqrt{\Gamma^{(0)}(x_1', x_1', \tau)\Gamma^{(0)}(x_2', x_2', \tau)}$$

$$= \tilde{G}^{(\infty)}(x_1' - x_2', \bar{\omega})\hat{\mu}^{(\infty)}[(x_1' + x_2')/2, \tau]/\left[\hat{G}^{(\infty)}(0, \bar{\omega}) \sqrt{\hat{\mu}^{(\infty)}(x_1', \tau)\hat{\mu}^{(\infty)}(x_2', \tau)}\right]. \tag{D11}$$

Since $I^{(\infty)}$ (as well as R_1, R_2 and θ) is a slow function relative to $\mu^{(\infty)}$, then it follows from the properties of Fourier transform pairs that $\hat{\mu}^{(\infty)}$ is a slow function relative to $\hat{}^{(\infty)}$. The temporal Fourier transform in Eq. (D10) does not change this relationship so that we can assume that $\hat{G}^{(\infty)}(x_1' - x_2') = 0$ except over very small domains in which

$$\hat{\mu}^{(\infty)}[(x_1' + x_2')/2, \tau] \approx \hat{\mu}^{(\infty)}(x_1', \tau) \approx \hat{\mu}^{(\infty)}(x_2', \tau). \tag{D12}$$

Upon substituting from Eq. (D12) into Eq. (D11) we have

$$\gamma_\omega^{(0)}(x_1', x_2', \tau) = \gamma_\omega^{(0)}(x_1', x_2', 0) = \hat{G}^{(\infty)}(x_1' - x_2', \bar{\omega})/\hat{G}^{(\infty)}(0, \bar{\omega}), \tag{D13}$$

so that upon substituting from Eq. (D2), and inverting the Fourier transform Eq. (D13) becomes

$$I(Rs) = G_0(\cos^2 \theta/\lambda^2 R^2) \iint_{-\infty}^{\infty} g(x_-', \omega) \exp(-iks \cdot x_-')d^2x_-', \tag{D14}$$

36

where $G_0 = \hat{G}^{(\infty)}(0, \omega)$ is a constant and

$$g(\mathbf{x}_1' - \mathbf{x}_2', \omega) \triangleq \gamma_\omega^{(0)}(\mathbf{x}_1', \mathbf{x}_2', 0),$$

$$\text{iffi } |\mathbf{x}_1'| \leq a \text{ and } |\mathbf{x}_2'| \leq a,$$

$$= 0 \text{ otherwise,} \tag{D15}$$

is a stationary correlation coefficient. Equation (55) follows by comparing Eq. (D14) to Eq. (52) by using Eqs. (D11) and (D15). Since the function $\gamma_\omega^{(0)}$ can be measured only over the portion of the $z = 0$ plane that is inside of the circle of radius a it is necessary to define g to be zero for $|\mathbf{x}_1' - \mathbf{x}_2'| > a$ to invert the Fourier transform in Eq. (D13) to obtain Eq. (D14).

Appendix E

CALCULATION LEADING TO EQUATION (60)

The derivation of Eq. (60) is virtually identical to that of Eq. (55) except for one slightly different assumption and some different coordinates and factors. The cross-spectral density function over the antenna hemisphere in Fig. 11 is given by

$$W_\omega^{(\infty)}(R_1 s_1, R_2 s_2) = (k/2\pi)^2 (\cos \theta_1 \cos \theta_2 / R_1 R_2) \exp [ik(R_1 - R_2)$$

$$\times \hat{I}(s_1 - s_2, \omega) \hat{\mu} [(s_1 + s_2)/2, \omega], \tag{E1}$$

where

$$\hat{I}^{(0)}(s_-, \omega) = \iint_{-\infty}^{\infty} I^{(0)}(x', \omega) \exp (-iks_- \cdot x') d^2x', \tag{E2}$$

and

$$\hat{\mu}^{(0)}(s_+, \omega) = \iint_{-\infty}^{\infty} \mu^{(0)}(x_-, \omega) \exp (-iks_+ \cdot x_-) d^2x_- \tag{E3}$$

(see Section 2, Eqs. (33), (34), and (35)), where $I^{(0)}$ is the intensity distribution over the $z = 0$ source plane, and $\mu^{(0)}$ is the complex degree of spectral coherence over the source plane. Equations (E1) through (E3) are different from Eqs. (D1) through (D3), but this does not affect the derivation of Eq. (60) in general.

Again as in Appendix D we assume that the source is quasi-homogeneous so that $I^{(0)}$ is a slow function relative to $\mu^{(0)}$. The derivation then proceeds just as in Appendix D, with the same assumptions, until we come to the requirement that the antenna plane be restricted so that Eq. (D8) is satisfied. Instead of the assumption given by Eq. (D8) we must make the similar assumption that $I^{(0)}$ vanishes outside of the domain where

$$|x'| << (\pi c/\Delta\omega). \tag{E8}$$

With this assumption, and with the assumption that the source intensity $I^{(0)}$ is effectively constant over the frequency domain passed by the receivers, we may remove $I^{(0)}(s, \bar{\omega})$ from the integration over ω' as we removed $\hat{G}^{(\infty)}$ from a similar integral in Appendix D.

The derivation then proceeds as before until we finally obtain instead of Eq. (D14)

$$I^{(0)}(x', \omega) = I_0/\lambda^2 \iint_{-\infty}^{\infty} g'(s_-) \exp (iks_- \cdot x') d^2s_-, \tag{E14}$$

39

where, instead of Eq. (D15),

$$g'(\mathbf{s}_1 - \mathbf{s}_2) \triangleq \Gamma^{(\infty)}(R_1\mathbf{s}_1, R_2\mathbf{s}_2, 0) \exp[-ik(R_1 - R_2)]/\sqrt{\Gamma^{(\infty)}(R_1\mathbf{s}_1, R_1\mathbf{s}_1, 0)\Gamma^{(\infty)}(R_2\mathbf{s}_2, R_2\mathbf{s}_2, 0)},$$

$$\text{iffi } s_{1x}^2 + s_{1y}^2 \leq 1 \text{ and } s_{2x}^2 + s_{2y}^2 \leq 1,$$

$$\triangleq 0 \text{ otherwise}, \tag{E15}$$

is a stationary correlation coefficient, and where I_0 is a constant given by

$$I_0 = \iint\limits_{-\infty}^{\infty} I^{(0)}(\mathbf{x}', \omega) d^2\mathbf{x}'. \tag{E16}$$

By comparison of Eqs. (E14) and (E15) with Eqs. (58) and (59) it is clear that they are equivalent if g' is given by Eq. (60). Because g' is defined physically only for unit vectors $\mathbf{s}_1$ and $\mathbf{s}_2$ pointing from the origin toward the $z \geq 0$ half space so that $s_{1x}^2 + s_{1y}^2 \leq 1$, and $s_{2x}^2 + s_{2y}^2 \leq 1$, it is necessary to define $g' = 0$ for all other values of s_{1x}, s_{1y} and s_{2x}, s_{2y} as indicated in Eq. (E15) to invert a Fourier transform to obtain Eq. (E14).